Journal of Molecular Graphics and Modelling 51 (2014) 50–63

Contents lists available at ScienceDirect

Journal of Molecular Graphics and Modelling

journal homepage: www.elsevier.com/locate/JMGM

Mechanistic investigation of the reactivity of disilene with nitrous oxide: A DFT study

Bholanath Maity, Debasis Koley*

Department of Chemical Sciences, Indian Institute of Science Education and Research (IISER) Kolkata, Mohanpur Campus, Mohanpur 741252, India

ARTICLE INFO

Article history:
Accepted 26 April 2014
Available online 5 May 2014

Keywords:
Disilene
Silylene
Nitrous oxide
Reactivity
DFT

ABSTRACT

We have reported the mechanistic investigation of the reaction of N_2O addition to disilene, *trans*-[$(TMS)_2N(\eta^1\text{-}Me_5C_5)Si{=}Si(\eta^1\text{-}Me_5C_5)N(TMS)_2$] ($\mathbf{1_t}$), employing density functional theory (BP86/TZVP//BP86/SVP) calculations. The potential energy surfaces of the title reaction are broadly classified under three pathways. Pathway I deals with the direct N_2O additions to $\mathbf{1_t}$ affording the *trans*-dioxadisiletane ring compound $\mathbf{P_t}$ whereas in the same pathway we report a different bifurcation route from intermediate $\mathbf{2_t}$. This route portrays the isomerization of *trans*-monooxadisiletane species $\mathbf{2_t}$ prior to the second N_2O addition, finally leading to the *cis*-isomeric product $\mathbf{P_c}$. Different possibilities for isomerization of disilene $\mathbf{1_t}$ to $\mathbf{1_c}$ were studied in pathway II. The *cis*-disilene ($\mathbf{1_c}$) formed can subsequently react with two N_2O molecules affording the *cis*-product $\mathbf{P_c}$. Pathway III details the formation of silanone type intermediate **6**, which subsequently combine with another silanone to afford loosely bound intermediates **7** and **8** respectively. The two separated silanone fragments in the isomeric intermediates **7** and **8** can then dimerizes to furnish the desired products. Among all the calculated potential energy surfaces, pathway III remains the most preferred route for disilene oxygenation under normal experimental condition. The present investigation about disilene reactivity will provide a deeper understanding on silylene chemistry and will exhibit promising applicability in main group chemistry as a whole.

1. Introduction

Disilenes, the compounds having silicon–silicon double bond, have gained considerable interest among chemists since its first isolation by West et al. [1]. The rich chemistry of disilene both in terms of bonding and reactivity has intensively been studied during the last few decades [2]. The highly reactive silylenes are the precursors to the formation of disilenes. The equilibrium that exists between the monomeric silylenes and its corresponding disilenes are subject to various experimental and theoretical studies. However, few examples are known where such dissociation equilibrium of the disilene with the silylene is observed. The thermal dissociation of extremely hindered and kinetically stable disilene into silylene under mild conditions was first reported by Okazaki et al. [3]. The existence of thermal dissociation was further supported by Tsutsui et al. by performing trapping experiments and DFT calculations [4]. Spectroscopic evidence for the existence of the silylene in equilibrium with the corresponding disilene at low temperature was reported by Kira and co-workers [5]. Later, West and Apeloig have reported the existence of dynamic equilibrium between *Z*-diaminodisilyldisilene and diaminosilylene by NMR and UV–vis spectroscopy [6]. The same authors have shown that two molecules of the saturated diaminosilylene initially undergo an insertion reaction leading to an intermediate silylene, which later dimerizes to the novel *Z*-diaminodisilyldisilene [6]. Recently, Jutzi, Scholler et al. described an unique situation where both the silylene [$(TMS)_2N(\eta^1\text{-}Me_5C_5)Si$] and its corresponding disilene *trans*-[$(TMS)_2N(\eta^1\text{-}Me_5C_5)Si{=}Si(\eta^1\text{-}Me_5C_5)N(TMS)_2$]($\mathbf{1_t}$) are stable and isolable under normal conditions and their reversible transformation can be realized by phase transfer [7]. They rationalized this fascinating behavior with steric strain and bonding flexibility (σ and π) of silicon bound pentamethylcyclopentadienyl (Cp^*) substituent. In 2011, Roesky and co-workers, have resynthesized the same disilene ($\mathbf{1_t}$, see Scheme 1) investigated previously by Jutzi et al. with a new method and enhanced yield [8]. Furthermore, the same authors have extended their effort in studying the reactivity of disilene $\mathbf{1_t}$ with various molecules including nitrous oxide (N_2O), elemental sulfur (S_8) and red phosphorus (P_4) [9]. It was observed that the reaction of $\mathbf{1_t}$ with N_2O at room temperature afforded both the *cis*- and *trans*- isomers of the dioxadisiletane

* Corresponding author. Tel.: +91 8902326716.
E-mail address: koley@iiserkol.ac.in (D. Koley).

http://dx.doi.org/10.1016/j.jmgm.2014.04.011
1093-3263/

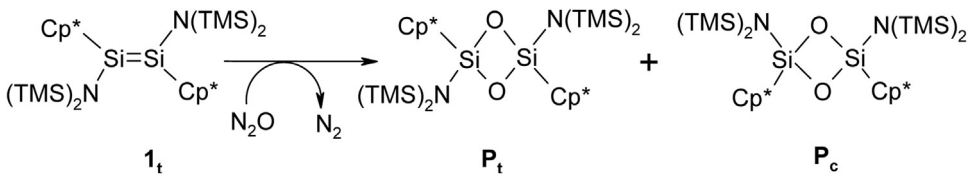

Scheme 1. Nitrous oxide addition to disilene $\mathbf{1}_t$.

ring compounds ($\mathbf{P_t}$ and $\mathbf{P_c}$ in Scheme 1). This is the first report where both the isomers are isolated and characterized from the same precursor disilenes.

Though there has been a dramatic increase in the understanding of chemistry, particularly the structural aspects, of disilenes; their reactivity and underlying mechanism are not fully explored [2,10]. Theoretical studies have provided conceptual insights on structure and bonding of silylenes and disilenes [11]. Mechanistic details of the disilene reactivity, particularly the addition reactions of water, alcohols, substituted phenols and halides were extensively explored in the group of Apeloig, Kira et al. [12]. Very recently, Su et al. performed DFT calculations to study the reactivity pattern of phosphino substituted dimetalalkenes containing M=M double bonded species (M = group 14 elements) to various types of chemical reactions *viz.* rearrangement reaction, 1,2 addition, transition metal complexation and [2 + 2] cycloaddition reaction [13]. Additionally, they have performed similar mechanistic studies on the reactivity patterns of fused tricyclic and cyclic dimetallenes of group 14 elements [14].

Presently we are interested in understanding the reactivity of $\mathbf{1_t}$ with N_2O as sketched in Scheme 1. N_2O, though found in traces, is nearly 300 times more potent as a greenhouse gas than CO_2 [15]. The importance of N_2O is significant as Nature uses nitrous oxide reductase (N_2OR) in the final step of the microbial denitrification process converting N_2O to dinitrogen and water [16]. Although substantial amount of research has been performed to understand the reactivity of N_2O in presence of transition metals [17], there are few literatures known to date where the N_2O activation is performed with multiple bonded main group compounds.

The main aim of this study is to undergo computational investigation on the mechanism of the reaction portrayed in Scheme 1. Furthermore, we were intrigued by the question about why and how the *cis*-product $\mathbf{P_c}$ is formed from the *E*-disilene precursor $\mathbf{1_t}$. Does the isomerization occurs prior to the N_2O addition or *vice versa*? To the best of our knowledge, no theoretical studies have been devoted to investigate the dimerization mechanisms of disilenes and pathways emanating from N_2O addition. Hence calculating the reaction pathways for the given reaction, particularly identifying the transition states and intermediates will certainly be of great theoretical interest.

2. Computational details

All calculations were performed using the Gaussian03 [18] and Gaussian09 quantum codes [19]. The geometries of all the intermediates and transition states are optimized with the generalized gradient approximation (GGA) to DFT by using the exchange functional of the Becke [20] in addition with the correlation functional of Perdew [21] (BP86). All the atoms are treated with Ahlrich's split valence plus polarization (SVP) basis sets [22] of 6-31G* quality. In all our DFT treatments, the resolution-of-the-identity (RI) approximation (also called "density fitting") for the two electron integrals was employed [23]. Further, spin unrestricted formalism (UBP86) was used for both open-shell singlet and triplet species. Transition states were located from a linear transit scan in which the reaction coordinate was kept fixed at different distances while all other degrees of freedom were optimized. After the linear transit search the transition states were optimized using the default Berny algorithm implemented in the Gaussian code [18,19]. In critical cases, the nature of a given transition state was analyzed by IRC (Intrinsic Reaction Coordinate) computations.

For further validation, single-point BP86 calculations ($E_e{}^L$) were performed on the BP86/SVP optimized geometries employing a valence triple-ζ type of basis set (TZVP) [24] incorporated in the Gaussian program suites [18,19]. To incorporate the dispersion effect, re-optimization of the BP86/SVP geometries were performed using the Grimme's dispersion corrected pure B97D [25] functional at SVP basis sets. Additional, single-point calculations ($^DE_e{}^L$) were performed at the optimized B97D/SVP geometries employing a higher TZVP basis set for all atoms. Single-point solvent calculations both at BP86/TZVP//BP86/SVP ($E_{sol}{}^L$) and B97D/TZVP//B97D/SVP ($^DE_{sol}{}^L$) levels were performed for all the intermediates and transitions states, using the SMD continuum solvation model [26] implemented in Gaussian09. Toluene was chosen as a solvent (dielectric constant $\varepsilon = 2.374$) with SMD-intrinsic Coulomb radii for the respective atoms. All single-point calculations were performed with tight wavefunction convergence criteria and "ultrafine" (99,950) grid was used in numerical integration. The different energy terms, $\Delta H_{298}{}^L$, $\Delta H_{sol}{}^L$, $\Delta G_{298}{}^L$ and $\Delta G_{sol}{}^L$ represented in Tables 2–4 (see text) are defined as follows. $\Delta H_{298}{}^L$ is the gas-phase enthalpy change where the total electronic energy at BP86/TZVP level is augmented with the enthalpy correction at BP86/SVP level. $\Delta H_{sol}{}^L$ is the solvent-phase enthalpy change where the total solvent electronic energy at BP86/TZVP level is augmented with the gas-phase enthalpy correction at BP86/SVP level. Similarly, $\Delta G_{298}{}^L$ is the gas-phase Gibbs free energy change where the total electronic energy at BP86/TZVP level is augmented with the free energy correction at BP86/SVP level. Finally, $\Delta G_{sol}{}^L$ is the solvent-phase free energy change where the total solvent electronic energy at BP86/TZVP level is augmented with the gas-phase free energy correction at BP86/SVP level.

To further check the effect of functional we have performed single-point calculations at M06-2X/TZVP level [24,27] on the B97D/SVP optimized geometries. The energies ($\Delta^{M06\text{-}2X}E_e{}^L$) are collected in Table S5 of the Supporting Information. The gas-phase TDDFT [19] singlet excitation energies of some selected species were calculated at BP86/TZVP level. In the calculation of the optical spectra, the 30 lowest spin-allowed singlet-singlet transitions were taken into account (see Supporting Information). The charge distribution was analyzed using the Weinhold's NPA (Natural Population Analysis) approach [28]. Figures are made from Chemcraft visualization program [29]. Calculations were performed in an octa-core, 64 bit Athlon workstation.

3. Results and discussion

In Table 1, we list the key geometrical features of the intermediates and transition states calculated in this present study. Schemes 2–4 sketches the desired reaction routes for the studied pathways. Figs. 1–3 depict their respective structures and Figs. 4–6 represents the energy profiles of the calculated pathways. Tables 2–4 documents the relative energies at BP86/TZVP//BP86/SVP level. The relative energies discussed in the

Table 1
Selected geometrical parameters at BP86/SVP level for all the structures involved in the investigated pathways. Distances are in angstroms (Å) and angle in degrees (°).

No.	r(Si1Si2)	r(Si1N1)	r(Si1C1)	r(Si1O1/ Si1O2)	r(Si2N2)	r(Si2C2)	r(Si2O2/ Si2O1)	θ_1[a]	θ_2[a]	Φ_1[a]	Φ_2[a]
$\mathbf{1_t}$	2.239	1.787	2.003	–	1.786	2.008	–	–	–	−1.1	−1.3
$\mathbf{[1_t\text{-}2_t]^‡}$	2.363	1.787	2.009	3.158/–	1.788	2.012	–/2.357	48.0	–	8.9	16.0
$\mathbf{2_t}$	2.305	1.771	1.993	1.753/–	1.770	1.992	–/1.753	82.2	–	−2.3	1.7
$\mathbf{[2_t\text{-}P_t]^‡}$	2.490	1.765	1.981	1.737/ 2.482	1.767	1.993	2.687/ 1.747	91.2	57.4	−7.3	−17.9
$\mathbf{P_t}$	2.492	1.756	1.954	1.734/ 1.732	1.756	1.954	1.734/ 1.732	91.9	91.9	−0.1	−0.1
$\mathbf{[2_t\text{-}3_t]^‡}$	3.111	1.729	1.903[c]	1.616/–	1.838	2.116	–/1.932	122.2	–	1.7	−8.6
$\mathbf{3_t}$	3.304	1.734	1.857[c]	1.624/–	1.824	2.081	–/1.841	144.7	–	35.2	24.3
$\mathbf{3_c}$	3.381	1.774	2.015	1.694/–	1.773	2.014	–/1.693	173.1	–	21.0[b]	20.7[b]
$\mathbf{[3_c\text{-}4_c]^‡}$	3.207	1.823	2.094	2.002/–	1.718	1.937	–/1.600	125.3	–	37.5[b]	7.9[b]
$\mathbf{4_c}$	2.339	1.777	2.001	1.756/–	1.778	2.001	–/1.749	83.6	–	16.9[b]	16.4[b]
$\mathbf{[4_c\text{-}P_c]^‡}$	2.476	1.779	1.986	1.748/ 2.329	1.767	2.026	2.847/ 1.738	90.5	56.0	10.3[b]	−6.4[b]
$\mathbf{P_c}$	2.492	1.754	1.951	1.736/ 1.739	1.766	1.965	1.728/ 1.726	92.0	91.8	2.9[b]	2.2[b]
$\mathbf{[1_t\text{-}2c_m]^‡}$	5.809	1.796	2.129	–	1.795	2.132	–	–	–	−170.3	−159.1
$\mathbf{2c_m}$	–	1.797	2.132[c]	–	–	–	–	–	–	–	–
$\mathbf{1_c}$	2.302	1.792	2.032	–	1.792	2.032	–	–	–	4.4[b]	4.3[b]
$\mathbf{[1_c\text{-}4_c]^‡}$	2.376	1.791	2.019	2.282/–	1.790	2.017	–/3.547	41.4	–	−10.3[b]	−4.7[b]
$\mathbf{[1_t\text{-}1_c]^‡}$	2.876	1.789	2.046	–	1.814	2.073	–	–	–	−127.7	−46.3
$\mathbf{[2c_m\text{-}5]^‡}$	–	1.778	2.110[c]	3.534	–	–	–	–	–	–	–
5	–	1.745	1.967[c]	3.127	–	–	–	–	–	–	–
6	–	1.745	1.975[c]	1.568	–	–	–	–	–	–	–
7	5.115	1.748	1.954[c]	1.572/4.237	1.748	1.953[c]	1.572/4.238	115.5	115.5	180.0	180.0
8	5.363	1.747	1.942[c]	1.572/4.532	1.736	2.018[c]	1.571/4.514	114.6	113.8	145.5[b]	129.5[b]

[a] (θ_1 = ∠Si1O1Si2; θ_2 = ∠Si1O2Si2; Φ_1 = ∠C1Si1Si2C2; Φ_2 = ∠N1Si1Si2N2).
[b] (Φ_1 = ∠C1Si1Si2N2; Φ_2 = ∠N1Si1Si2C2).
[c] Distance between Si and center-of-mass of the coordinated η^2 carbons of the Cp* ring.

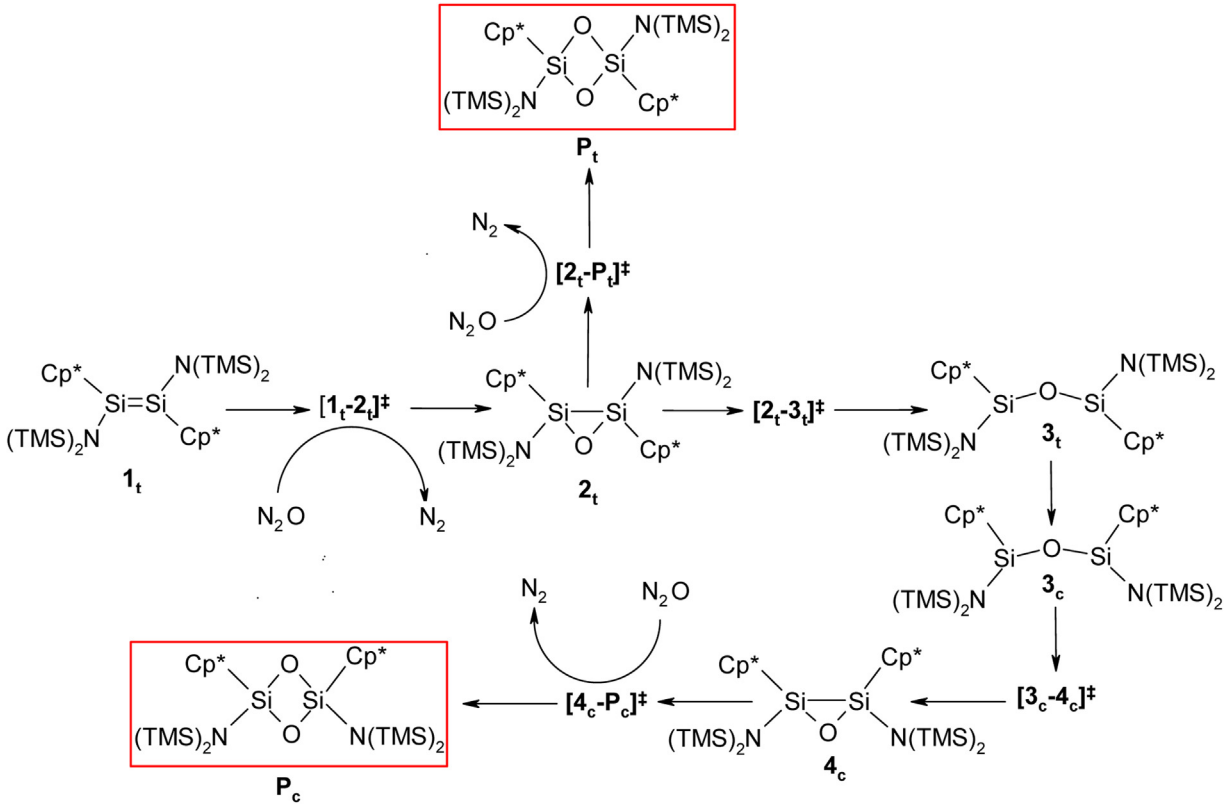

Scheme 2. Reaction steps involved in pathway I.

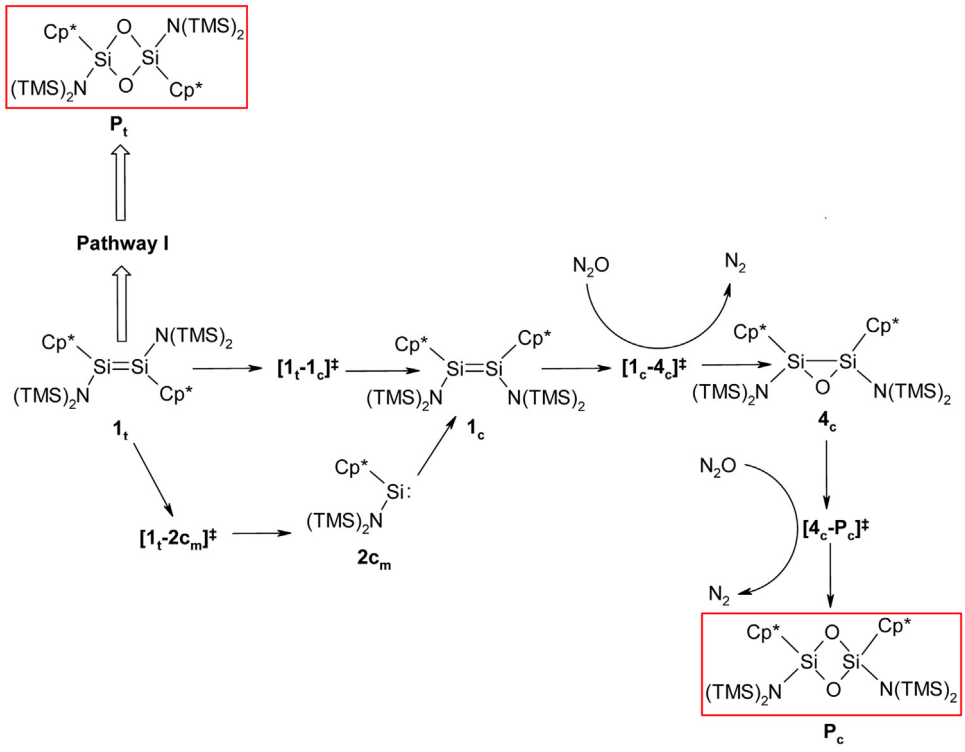

Scheme 3. Reaction steps involved in pathway II.

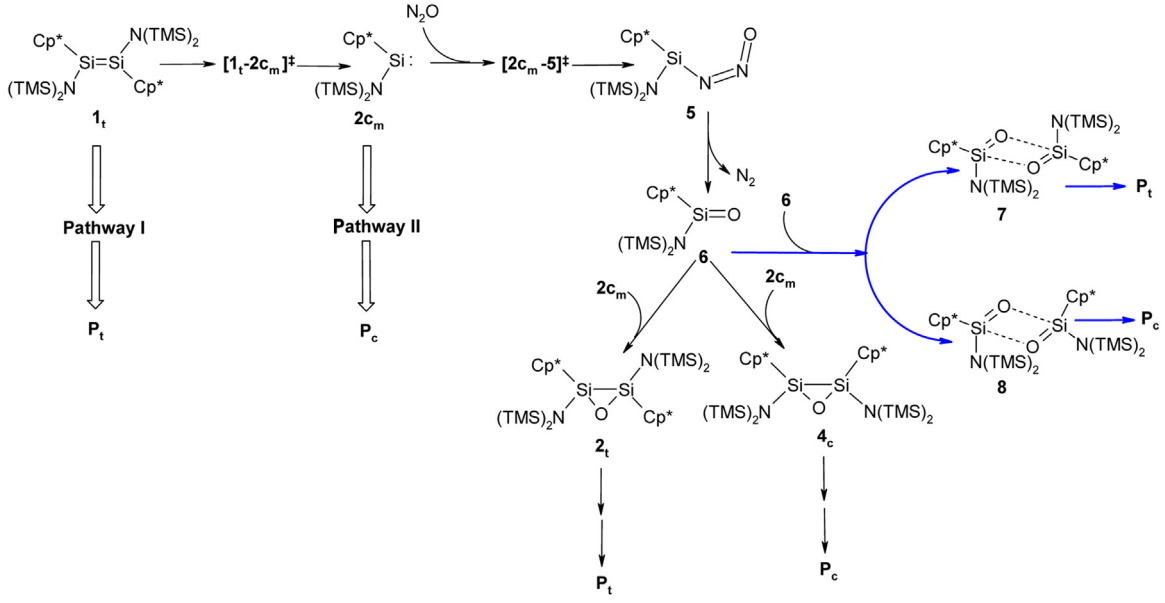

Scheme 4. Reaction steps involved in pathway III.

Table 2
Energies (in kcal/mol) for all the steps (refer Scheme2) involved in the pathway I. For different energy terms refer computational details.

Steps	$\Delta H_{298}{}^{L}$	$\Delta H_{sol}{}^{L}$	$\Delta G_{298}{}^{L}$	$\Delta G_{sol}{}^{L}$
$\mathbf{1_t} \rightarrow \mathbf{[1_t\text{-}2_t]^{\ddagger}}$	25.2	24.1	33.8	32.8
$\mathbf{[1_t\text{-}2_t]^{\ddagger}} \rightarrow \mathbf{2_t}$	−131.9	−129.6	−138.6	−136.3
$\mathbf{2_t} \rightarrow \mathbf{[2_t\text{-}P_t]^{\ddagger}}$	31.2	30.7	40.3	39.7
$\mathbf{[2_t\text{-}P_t]^{\ddagger}} \rightarrow \mathbf{P_t}$	−150.5	−148.6	−160.8	−158.9
$\mathbf{2_t} \rightarrow \mathbf{[2_t\text{-}3_t]^{\ddagger}}$	28.3	25.2	24.5	21.5
$\mathbf{[2_t\text{-}3_t]^{\ddagger}} \rightarrow \mathbf{3_t}$	−2.9	−1.8	−1.6	−0.5
$\mathbf{3_t} \rightarrow \mathbf{3_c}$	1.9	3.5	-0.1	1.5
$\mathbf{3_c} \rightarrow \mathbf{[3_c\text{-}4_c]^{\ddagger}}$	6.9	5.7	7.1	5.9
$\mathbf{[3_c\text{-}4_c]^{\ddagger}} \rightarrow \mathbf{4_c}$	−24.6	−22.7	−22.2	−20.3
$\mathbf{4_c} \rightarrow \mathbf{[4_c\text{-}P_c]^{\ddagger}}$	30.5	30.3	41.3	41.1
$\mathbf{[4_c\text{-}P_c]^{\ddagger}} \rightarrow \mathbf{P_c}$	−155.9	−154.4	−164.0	−162.5

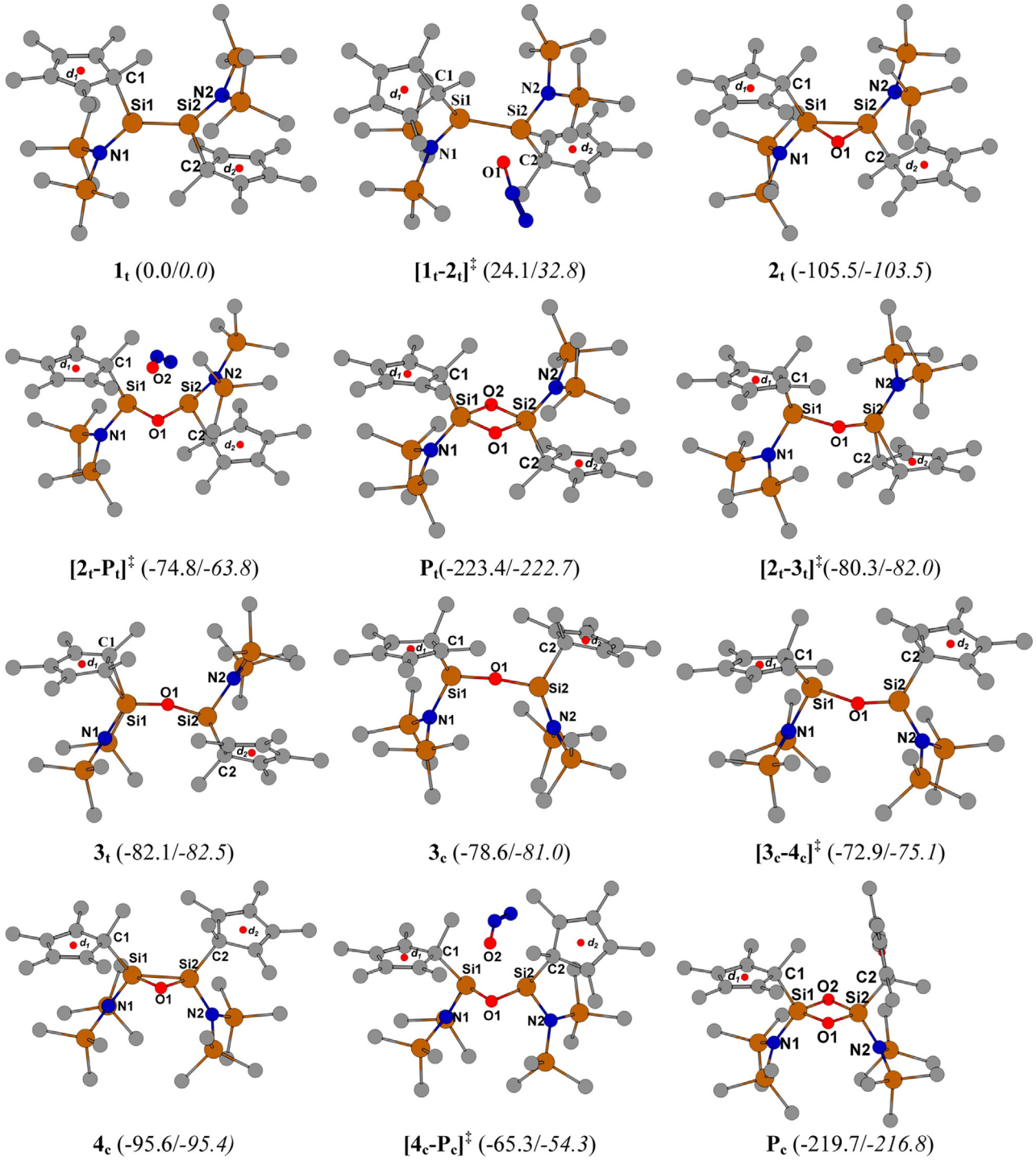

Fig. 1. BP86/SVP optimized geometries of the intermediates and transition states involved in the pathways I and II respectively. Hydrogens are omitted for clarity. Color code: C: gray; Si: brown; N: blue; O: red. The smaller red dots d_1 and d_2 represents the center-of-mass of the Cp* rings. The values in parentheses are $\Delta H_{sol}{}^{L}/\Delta G_{sol}{}^{L}$ in kcal/mol relative to the starting material $\mathbf{1}_t$ at BP86/TZVP//BP86/SVP level.

text will be $\Delta H_{sol}{}^{L}$ and $\Delta G_{sol}{}^{L}$ (refer computational details) if not otherwise stated.

The different reaction channels that are investigated for the N_2O addition are designated as pathway I, II and III respectively, which will be discussed in a point wise manner.

3.1. Pathway I

This pathway will discuss the formation of both *trans*- and *cis*-dioxadisiletane ring products $\mathbf{P_t}$ and $\mathbf{P_c}$ from *trans*-monooxadisiletane intermediate $\mathbf{2_t}$. Complete schematic representation of pathway I is depicted in Scheme 2. BP86/SVP optimized $\mathbf{1_t}$ shows a strong structural resemblance with the X-ray crystal structure as seen from the alignments and superposition of the respective structures (see Figure S1) [8]. Jutzi et al. reported that the short Si1=Si2 double bond (2.239 Å, refer Table 1) induces some steric strain within the molecule that causes deviations of bond lengths and bond angles of the bulky substituent's [7]. The calculated degree of *trans*-pyramidalization (21.7° and 21.8°, the angle between the Si1—S12

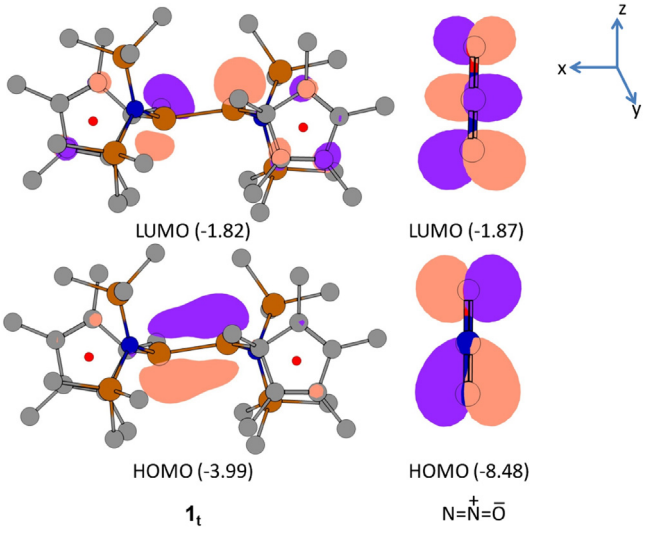

Fig. 2. Frontier molecular orbitals of $\mathbf{1}_t$ and N_2O (isodensity = 0.03 electron/bohr^3). The values in parentheses represent orbital eigenvalues in eV.

vector and the SiL_2 plane) at BP86/SVP level is comparatively higher than the crystal structure values (8.9° and 10.6°), suggesting a more planar geometry due to crystal structure packing [2d,7,8,].

Table 3
Energies (in kcal/mol) for all the steps involved in the pathway II. For different energy terms refer computational details.

Steps	$\Delta H_{298}{}^L$	$\Delta H_{sol}{}^L$	$\Delta G_{298}{}^L$	$\Delta G_{sol}{}^L$
$\mathbf{1_t \rightarrow [1_t\text{-}2c_m]^{\ddagger}}$	16.9	15.3	10.7	9.2
$\mathbf{[1_t\text{-}2c_m]^{\ddagger} \rightarrow 2c_m}$	−3.4	−6.2	−15.7	−18.6
$\mathbf{2c_m \rightarrow 1_c}$	−5.2	−1.1	12.6	16.7
$\mathbf{1_c \rightarrow [1_c\text{-}4_c]^{\ddagger}}$	20.5	20.1	32.0	31.6
$\mathbf{[1_c\text{-}4_c]^{\ddagger} \rightarrow 4_c}$	−126.0	−123.7	−136.6	−134.3
$\mathbf{1_t \rightarrow [1_t\text{-}1_c]^{\ddagger}}$	24.7	23.7	22.7	21.8
$\mathbf{[1_t\text{-}1_c]^{\ddagger} \rightarrow 1_c}$	−16.4	−15.7	−15.2	−14.5

Table 4
Energies (in kcal/mol) for all the steps involved in the pathways III. For different energy terms refer computational details.

Steps	$\Delta H_{298}{}^L$	$\Delta H_{sol}{}^L$	$\Delta G_{298}{}^L$	$\Delta G_{sol}{}^L$
$\mathbf{2c_m \rightarrow [2c_m\text{-}5]^{\ddagger}}$	7.2	6.5	16.8	16.1
$\mathbf{[2c_m\text{-}5]^{\ddagger} \rightarrow 5}$	−12.4	−15.6	−11.7	−14.8
$\mathbf{5 \rightarrow 6}$	−81.2	−77.6	−90.0	−86.4
$\mathbf{6 \rightarrow 4_c}$	−24.3	−18.1	−7.0	−0.9
$\mathbf{6 \rightarrow 2_t}$	−33.8	−28.0	−14.8	−9.0
$\mathbf{6 \rightarrow 7}$	2.7	6.7	13.9	17.9
$\mathbf{6 \rightarrow 8}$	0.8	4.5	12.1	15.8
$\mathbf{7 \rightarrow P_t}$	−69.4	−66.0	−64.3	−60.9
$\mathbf{8 \rightarrow P_c}$	−67.5	−63.7	−62.6	−58.8

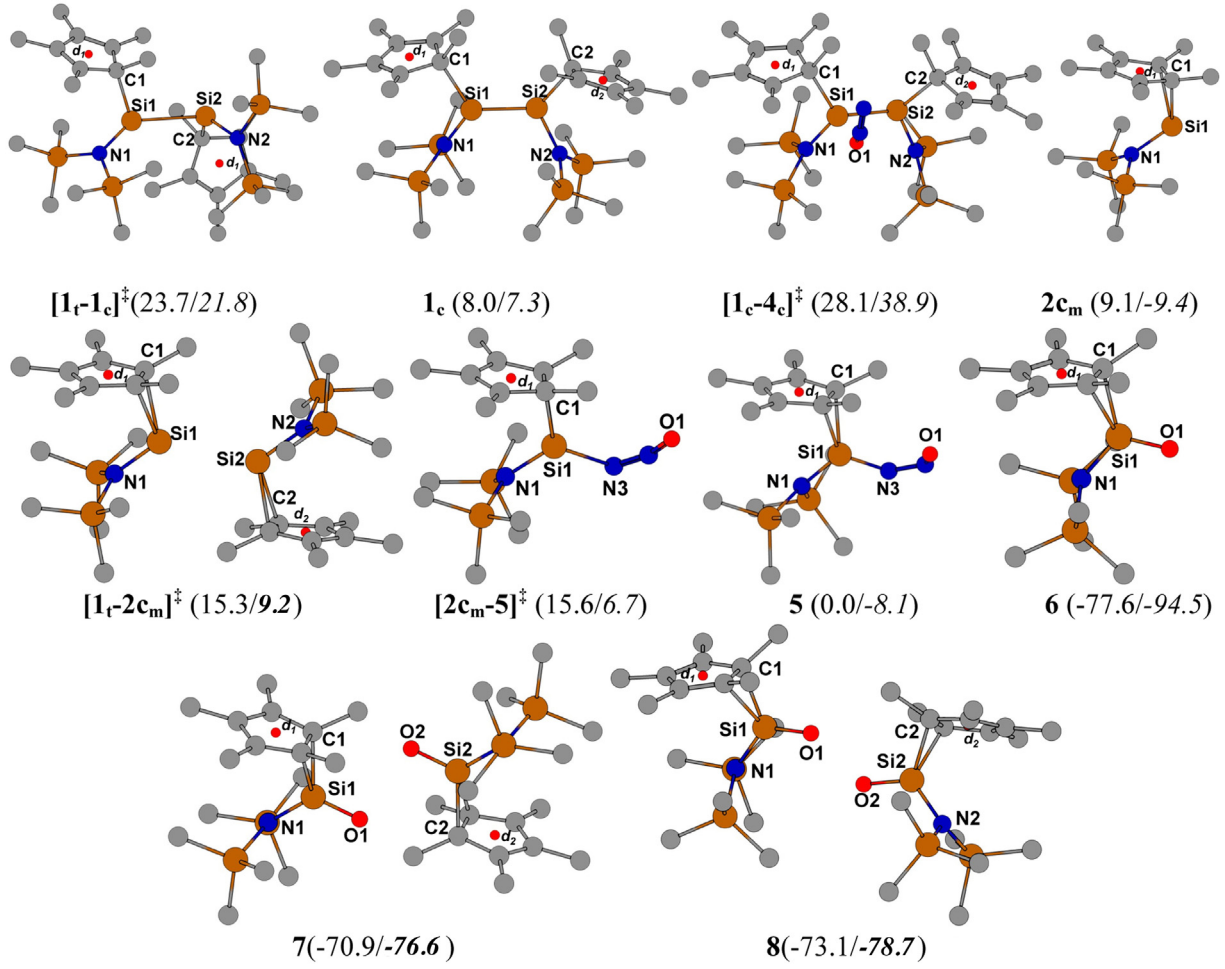

Fig. 3. BP86/SVP optimized geometries of the additional intermediates and transition states involved in the pathways II and III respectively. Hydrogens are omitted for clarity. Color code: C: gray; Si: brown; N: blue; O: red. The values in parentheses are $\Delta H_{sol}{}^L/\Delta G_{sol}{}^L$ in kcal/mol relative to the starting material $\mathbf{1}_t$ at BP86/TZVP//BP86/SVP level. (For interpretation of the references to color in this figure legend, the reader is referred to the web version of the article.)

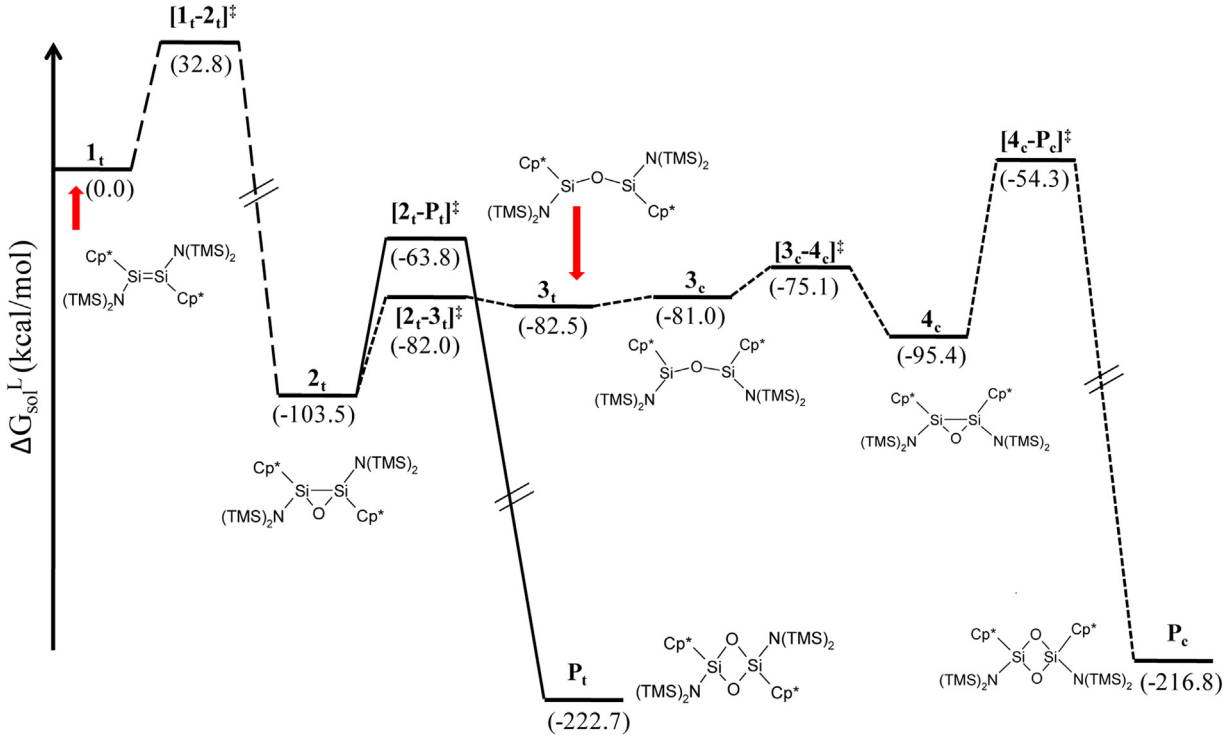

Fig. 4. Energy profile for pathway I. The solid line shows the profile for the step $\mathbf{2}_t \rightarrow \mathbf{P}_t$ (refer text). Energy values ($\Delta G_{sol}{}^{L}$, kcal/mol) in parentheses are relative to starting material $\mathbf{1}_t$.

West and coworkers have reported a strong absorption band at 420 nm for tetramesityldisilene, the first isolated disilene species [1]. The same authors assigned the peak to be π–π* type, which imparts a yellow color to the compound. Kira et al. have also reported an absorption band at 437 nm for tetraaminodisilene (i-$Pr_2N)_2Si{=}Si(NPr\text{-}i_2)_2$ species while studying the reversible equilibrium between silylene and disilene using spectroscopic techniques [5]. In $\mathbf{1_t}$ we observe a similar excitation at 437 nm,

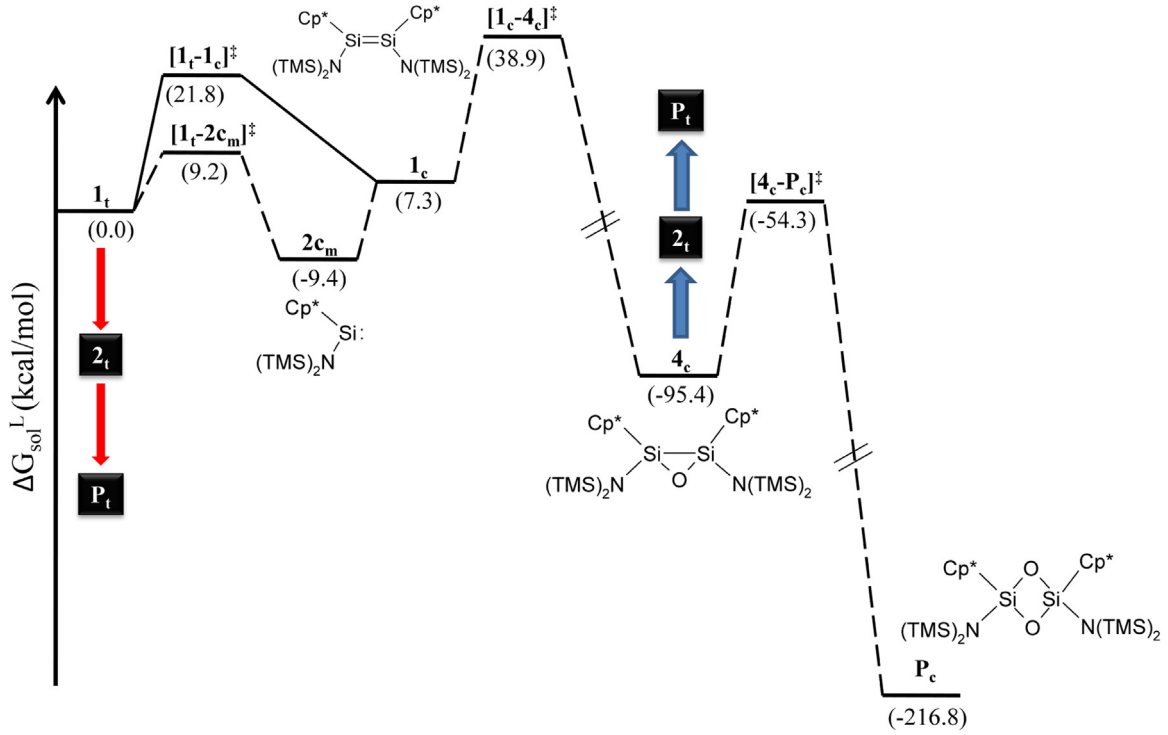

Fig. 5. Energy profile for pathway II. The solid line shows the profile for the step $\mathbf{1}_t \rightarrow \mathbf{1}_c$ *via* bond rotation (see text). Energy values ($\Delta G_{sol}{}^{L}$, kcal/mol) in parentheses are relative to starting material $\mathbf{1}_t$. Blue and red arrows shows connection channel to pathway I. (For interpretation of the references to color in this figure legend, the reader is referred to the web version of the article.)

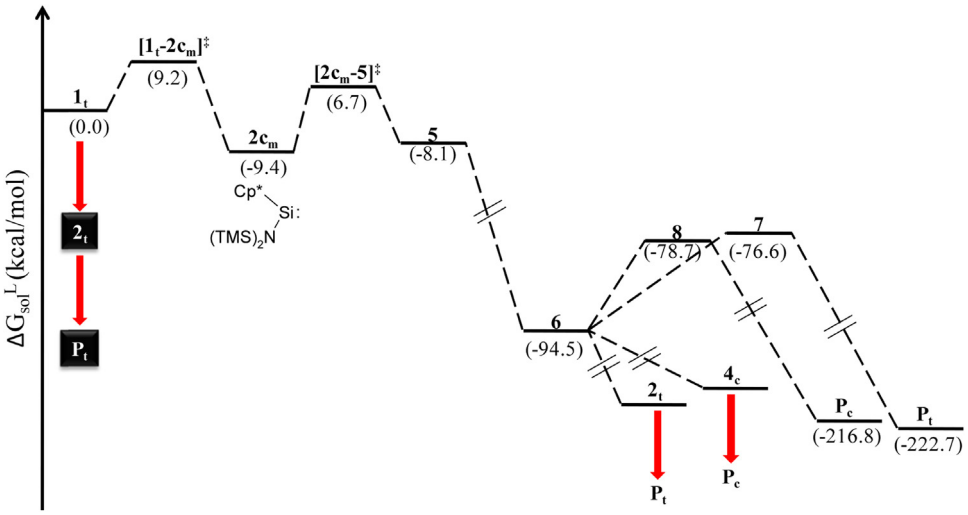

Fig. 6. Energy profile for pathway III. The arrows designate the entry routes for pathways I and II respectively. Energy values ($\Delta G_{sol}{}^{L}$, kcal/mol) in parentheses are relative to starting material $\mathbf{1}_t$.

with moderately high oscillator strength (*f*) of 0.125 (see Figure S3 and Table S7). The bathochromic shift of the π–π* transition in $\mathbf{1_t}$ compared to tetramesityldisilene originates from an extended conjugation between Cp* and Si1═Si2 orbitals, elevating the HOMO energy and reducing the π–π* energy difference. However, there is an additional low intensity excitation obtained at 511 nm. These two excitations are primarily π–π* in nature with HOMO, HOMO-2, LUMO and LUMO+1 show contributions from silicon atoms and Cp* moieties (refer Figure S2).

The first step toward the activation of $\mathbf{1_t}$ takes place in presence of a single N_2O molecule giving rise to *trans*-monooxadisiletane species $\mathbf{2_t}$ as shown in Scheme 2 and Fig. 4. In order to understand the reaction step $\mathbf{1_t} \rightarrow \mathbf{2_t}$ the N_2O molecule is required to advance toward $\mathbf{1_t}$ using a potential energy surface scan (PES). During such PES scan the oxygen atom of N_2O was allowed to approach uniformly toward both the silicon atoms (Si1 and Si2) in $\mathbf{1_t}$, however during the transition state optimization the N_2O shifts more closer to Si2 (Si2—O1 = 2.357 Å *vs.* Si1—O1 = 3.185 Å) than Si1. With further decrease in the O1—Si1(Si2) distances the N_2 unit from N_2O gets decoordinated with the formation of $\mathbf{2_t}$ [30]. We have not identified any weak van der Waals type pre-complex in the reaction step $\mathbf{1_t} \rightarrow \mathbf{2_t}$, like the one observed by Kira et al. during water addition to disilene [12a,b,e]. The silicon—oxygen distances in $\mathbf{[1_t\text{-}2_t]^{‡}}$ is relatively longer (Si2—O1 = 2.357 Å and Si1—O1 = 3.185 Å in $\mathbf{[1_t\text{-}2_t]^{‡}}$ *vs.* Si1/Si2—O1 = 1.753 Å in $\mathbf{2_t}$) than the intermediate $\mathbf{2_t}$ suggesting a much earlier transition state along the reaction coordinate (refer Table 1).

The NPA group charge of N_2O in the transition state is 0.413 *e* indicating a charge transfer from the disilene $\mathbf{1_t}$ to the incoming N_2O moiety. The effect of such charge transfer is manifested with the elongation of the Si1—Si2 bond distance in $\mathbf{[1_t\text{-}2_t]^{‡}}$ by 0.124 Å with respect to the reactant $\mathbf{1_t}$ (Table 1). This observation can be explained on the basis of FMO (Frontier Molecular Orbital) theory [31] where electrophilic interaction occurs between the π HOMO of $\mathbf{1_t}$ and π* LUMO of N_2O during the initial encounter of the two moieties (refer Fig. 2). However, similar electrophilic addition to disilene is not obscure. Apeloig and Nakash have shown that the addition of phenols carrying electron withdrawing substituent (*e.g.* *p*-$F_3CC_6H_4OH$) to bulky disilene (Mes_2Si═$SiMes_2$, Mes = mesityl) is accompanied with a rate-determining electrophilic step, where the phenolic hydrogen gets coordinated to the unsaturated silicon atom [12f,g,h]. The reaction energy for the formation of $\mathbf{2_t}$ is both exothermic and exergonic at BP86/TZVP//BP86/SVP level ($\Delta H_{sol}{}^{L} = -105.5$ kcal/mol and $\Delta G_{sol}{}^{L} = -103.5$ kcal/mol) supporting a high irreversibility for this step. High exothermicity in the previous step is mainly due to the liberation of nitrogen and also from the fact that the weak Si═Si π bond is traded with the formation of strong Si—O—Si bridging bond. The transition state $\mathbf{[1_t\text{-}2_t]^{‡}}$ is characterized with an imaginary mode depicting the asynchronous coordination of O1 toward the Si2 atom. The activation barrier for the step $\mathbf{1_t} \rightarrow \mathbf{2_t}$ is 24.1 kcal/mol ($\Delta H_{sol}{}^{L}$, Table 2), which is within the range of values obtained by Su et al. while calculating the thermodynamics of the reactivity of strained cyclic dimetalalkenes with small molecules like water, methanol, acetone and diazene [13,14].

The structural feature of $\mathbf{2_t}$ is unique, comprising of a three member ring with two basal silicon atoms and a more electronegative oxygen atom at the apex (Fig. 1). The Si1—Si2 distance is 2.305 Å, which is even shorter than the Si—Si single bond distance (2.327 Å) in H_3Si—SiH_3 [32]. The origin of this unusual geometry and the inherent bonding of disilaoxirane and 1,3-cyclodisiloxane have been thoroughly investigated using theoretical methods in the groups of Schaefer, Allen, Kraka, Nagase, Inagaki and others [33].

The structure $\mathbf{2_t}$ formed will further react with another N_2O molecule to furnish the *trans* product $\mathbf{P_t}$. The second N_2O molecule approaches the silicon atoms from a site opposite to the previous one (Fig. 1). Most importantly, in the transition state $\mathbf{[2_t\text{-}P_t]^{‡}}$ the Si1—Si2 distance has elongated to 2.490 Å, which is 0.185 Å longer than at $\mathbf{2_t}$. This elongation is again an effect of charge transfer (0.465 *e*) from disilene fragment to the N_2O unit. At $\mathbf{[2_t\text{-}P_t]^{‡}}$ the O2 from the N_2O molecule is relatively closer to Si1 than Si2, (Si1—O2 = 2.482 Å *vs.* Si2—O2 = 2.687 Å) unlike the situation observed at $\mathbf{[1_t\text{-}2_t]^{‡}}$. The three-member Si1O1Si2 ring in $\mathbf{2_t}$ has equal Si1/Si2—O1 bond distances (1.753 Å, refer Table 1), which gets perturbed with the gradual progress of N_2O moiety. The Si1—O—Si2 bond angle in $\mathbf{[2_t\text{-}P_t]^{‡}}$ has widened ($\theta_1 = 82.2^{\circ}$ in $\mathbf{2_t}$ *vs.* 91.2° in $\mathbf{[2_t\text{-}P_t]^{‡}}$) allowing room for the second oxygen to coordinate resulting in a four member Si1O1Si2O2 ring. The free energy of activation for the transition $\mathbf{2_t} \rightarrow \mathbf{P_t}$ is 39.7 kcal/mol, which is 6.9 kcal/mol higher than the energy barrier involved in the previous reaction step ($\mathbf{1_t} \rightarrow \mathbf{2_t}$). Gratifyingly, the $\mathbf{[2_t\text{-}P_t]^{‡}}$ is more stabilized than $\mathbf{1_t}$ by −63.8 kcal/mol, allowing the transformation to be facile under experimental conditions. The activated complex $\mathbf{[2_t\text{-}P_t]^{‡}}$ is characterized with a single imaginary mode animating the approach of the incoming O2 toward the silicon atoms along with a concomitant elongation of the O2—N_2 bond. The formation of $\mathbf{P_t}$ is extremely exothermic and it is −222.7 kcal/mol stable than the starting material (refer Table 2). The BP86/SVP optimized structure $\mathbf{P_t}$ shows

strong resemblance with the solid state structure obtained by Roesky et al. [9] The Si1—Si2 distance in **P_t** has substantially increased (2.492 Å in **P_t** *vs.* 2.305 Å in **2_t**) with the addition of second oxygen atom to the three-member Si1O1Si2 ring in **2_t**. Unlike other dioxadisiletane ring compounds the O1—O2 non-bonded distance is shorter than the Si1—Si2 distance (O1—O2 = 2.408 Å) [33]. The main reason may be that apart from silicon having larger van der Waals radius, the two vicinal bulky bis(trimethylsilyl)amino [$(Me_3Si)_2N$] and pentamethylcyclopentadienyl substituent's refrain the oxygen atoms to come closer to each other (Fig. 1).

From **2_t** another reaction route emanates, leading to the formation of isomeric *cis*-dioxadisiletane product **P_c** (refer Scheme 2 and Fig. 4). The structure **2_t** so formed (*vide supra*) can undergo a series of transformation to furnish its *cis* variant **4_c** (refer Figs. 1 and 4). Gradual elongation of the Si1—Si2 distance in **2_t** will lead to **3_t**, where both the $(Me_3Si)_2N$ ligands are nearly *trans* to each other (∠N1—Si1—Si2—N2 = 155.7°). The interesting structural feature in **3_t** is the different mode of Cp* coordination to the Si atoms: η^2 with Si1 and η^1 with Si2 respectively (Fig. 1). Jutzi et al. have previously reported the effect of Cp* mode of bonding in understanding the reversible phase-dependent transformation between **1_t** and its monomeric silylene **$2c_m$** [7]. The Si2—O1 bond has elongated more than the Si1—O1 distance (Si1—O1 = 1.624 Å *vs.* Si2—O1 = 1.841 Å) in **3_t** indicating a more silanone type of character in the Si1—O1 bond (*vide infra*). The two Cp* rings are fully *trans* oriented with a tilt angle {∠C2Si2Si(center-of-mass of the η^2 carbons)} of 121.3°. The activation barrier for the process **$2_t \rightarrow 3_t$** is 21.5 kcal/mol, with the transition state **$[2_t\text{-}3_t]^‡$** depicting the correct imaginary mode of Si1—Si2 bond cleavage and a concomitant flattening of the Si—O1—Si2 angle. However, a similar transition state at B97D/SVP surface was not observed even after repeated attempts [34]. Under dispersion corrected energy surface, gradual elongation of Si1—Si2 distance in **2_t** directly furnished the intermediate **3_t**. The Si1—Si2 bond distance in **3_t** is 3.304 Å, which is lengthen by roughly 1.0 Å from **2_t** with an additional increase of Si1—O1—Si2 bond angle to 144.7° (Table 1). The Si1—O1—Si2 bond angle in **3_t** is much wider than in dimethyl ether (111.5°) [35a] but very similar to the simplest disiloxane $H_3Si—O—SiH_3$ (144.1°) [35b].

The **3_t** can subsequently isomerize to **3_c** by mere rotation along the relatively weaker Si2—O2 bond [36]. Bond rotation of similar fashion was reported by the groups of Kira and Apeloig while explaining the formation of different stereoisomeric products after addition of water/alcohols to disilenes.[12] Both the isomers are nearly isoenergetic with **3_t** about 1.5 kcal/mol stable than **3_c** (Table 2). Structure **3_c**, apart from its ligands being *cis* oriented, has perceptible geometrical differences compared to its immediate predecessor **3_t**. The Si1—Si2 distance has slightly elongated (3.381 Å in **3_c** *vs.* 3.304 Å in **3_t**) and there is an appreciable decrease in the Si2—O1 bond distance (1.693 Å in **3_c** *vs.* 1.841 Å in **3_t**). The Si1—O1 and Si2—O1 distances became similar compared to **3_t** and more importantly there is a substantial opening up of the Si1—O1—Si2 bond angle (refer Table 1).

We can envisage the formation of **4_c** only if the two silicon atoms in **3_c** undergo bond formation to furnish a similar three-member ring structure analogous to **2_t**. Gradual shortening of the Si1—Si2 distance resulted in the formation of **4_c** *via* the transition state **$[3_c\text{-}4_c]^‡$** (Fig. 4). The activation barrier for the process is 5.9 kcal/mol with the transition state eigenvector animating the desired atomic motions. Like **$[2_t\text{-}3_t]^‡$**, a similar transition state of the type **$[3_c\text{-}4_c]^‡$** was not observed at B97D/SVP level (*vide supra*).[34] There was a direct collapse of the intermediate **3_c** to **4_c** with gradual decrease of Si1—Si2 bond distance. The structure **4_c** is 8.1 kcal/mol less stable than **2_t**, such energy difference probably originates from the steric interaction of two bulky Cp* ligands. **4_c** will then interact with a second N_2O molecule resulting in the *cis*-product **P_c** (Fig. 4). The approach of second N_2O molecule to **4_c** is off-center with asynchronous distance of O2 with respect to Si1 and Si2 (Fig. 1). Like **$[2_t\text{-}P_t]^‡$** the O2 from N_2O is comparatively closer to Si1 than Si2 (Si1—O2 = 2.329 Å *vs.* Si2—O2 = 2.847 Å). A similar type of off-center attack of substituted germylene (GeR_2) to ethylene was reported and analyzed by Su and Chu using state-of-the-art theoretical methods [37]. The Si1—Si2 bond distance in **$[4_c\text{-}P_c]^‡$** has increased to 2.476 Å, again a manifestation of charge transfer (0.425 *e*) from the disilene unit to the N_2O moiety. The activation barrier for the transition **$4_c \rightarrow P_c$** is 41.1 kcal/mol that is comparable for the step **$2_t \rightarrow P_t$** (Table 2) leading to the *trans* product (*vide supra*). The **P_c** formed is -216.8 kcal/mol stable than the starting material **1_t**. Relative stability of both the isomeric products reveals that **P_t** is more stable than **P_c**, by 5.9 kcal/mol (Fig. 1). This calculated result is in accordance with the experimental findings from the group of Roesky [9a].

3.2. Pathway II

The E,Z-isomerization of disilenes has been explored since decades by various experimental groups using NMR and spectroscopic techniques [4,38]. However, to the best of our knowledge computational investigation of this unimolecular isomerization reaction for disilene **1_t** has not been undertaken. Kira et al. have pointed out that unlike olefins, where the rotation around the C=C double bond is energetically expensive (*ca.* 60 kcal/mol), isomerization of disilenes is facile [2d]. There are three different mechanisms reported for the isomerization of disilenes which are as follows: (1) rotation around the Si—Si bond, (2) dissociation of disilene into corresponding silylene and then further recombination and finally (3) 1,2-migration of the substituent leading to silysilylene derivatives [38b,2d]. Pathway II will elucidate the mechanistic channels for isomerization of **1_t** and its further addition of N_2O molecules to yield the dioxadisiletane ring product (Scheme 3 and Fig. 5).

Dissociation of **1_t** leads to the formation of monomeric species **$2c_m$** (Fig. 5). Since **1_t** has strong steric crowding among the substituents, dispersion corrected DFT energies will be more reliable in accounting the inherent van der Waals interaction present in the species. The bond dissociation energy was calculated to be 37.0 kcal/mol ($\Delta^D E_e{}^L$, Table S5), a similar value was previously reported by Jutzi et al. for the same disilene species **1_t** [7]. Interestingly, the dispersion included Gibbs free energy value for **1_t** dissociation indicates that the silylene formation in toluene is more favorable than in gas-phase ($\Delta^D G_{298}{}^L = 10.2$ *vs* $\Delta^D G_{sol}{}^L = -2.9$ kcal/mol, Table S5). The monomeric silylene **$2c_m$** is more polar than **1_t** since it has a higher dipole moment value (μ_D = 1.467 D for **$2c_m$** and 0.179 D for **1_t**) and hence will be more stabilized under condensed phase.

The dissociation of **1_t** is associated with an activation barrier of 9.2 kcal/mol (Fig. 5, Table 3), which can be accessed under the reaction condition. In **$[1_t\text{-}2c_m]^‡$**, the disilene has already been dissociated with the Si1—Si2 distance of 5.809 Å and the silicon atoms are coordinated with the Cp* units in a η^2 fashion (Fig. 3). In fact a similar type of transition state was not identified at B97D/SVP level however a high lying intermediate was formed that is 10.4 kcal/mol ($\Delta^D G_{sol}{}^L$; refer Table S5) unstable than **1_t**. Complete separation of the silylene moieties from this intermediate is exergonic (-13.3 kcal/mol, $\Delta^D G_{sol}{}^L$) giving rise to two molecules of monomeric silylenes.

Silylene **$2c_m$** can further dimerize to afford the *cis* isomer **1_c**. Formation of **1_c** is exothermic ($\Delta^D E_e{}^L = -32.2$ kcal/mol, Table S5) but the entropic penalty for the recombination process allows the Gibbs free energy change to be less exoergic ($\Delta^D G_{298}{}^L = -5.4$ kcal/mol, Table S5). Another route for the formation of **1_c** will be a simple bond rotation around the Si=Si bond in **1_t** (*vide supra*). Rotation around Si1—Si2 bond in **1_t** resulted in **1_c** *via* the transition state **$[1_t\text{-}1_c]^‡$**, which was validated using an IRC calculation (see

computational details). The activation barrier for the process is 21.8 kcal/mol, the value is in accordance with the measured activation energies for the isomerization of various substituted disilenes [4,38]. The Si1—Si2 bond in **[1$_t$-1$_c$]**‡ has lengthened to 2.876 Å and the imaginary mode depicts the twisting mode of one of the Si(Cp*)(N(SiMe$_3$)$_2$) unit. Though the dihedral angle $\Phi_1 > \Phi_2$ (see Table 1) the average of the angles is approximately 93° indicating that the substituents in **[1$_t$-1$_c$]**‡ are oriented in between the *trans* and *cis* conformations (Figs. 1 and 3). To the best of our knowledge this is the first characterization of a transition state for disilene isomerization *via* Si=Si double bond rotation employing computational technique [39,40]. However there are reports stating that the twisted configuration of disilenes are stable at the triplet electronic state and such low lying triplet can lower the rotation barrier [38c, 41]. The optimized triplet state at the singlet transition state **[1$_t$-1$_c$]**‡ geometry was indeed more stable by 2.6 kcal/mol ($\Delta H_{298}{}^{L}$). The key geometrical parameters between the two electronic states do not vary significantly (Figure S5) except the dihedral angle (N1—Si1—Si2—N2) has increased to −74.4° and the Si1—Si2 distance has shortened to 2.419 Å (−46.3° and 2.876 Å in **[1$_t$-1$_c$]**‡).

The molecule **4$_c$**, formed from **2$_t$** through a series of conformational changes as reported in pathway I (*vide supra*), can also be obtained from **1$_c$** after addition of a single N_2O molecule (Scheme 3 and Fig. 5). The gradual approach of N_2O to **1$_c$** was performed in a similar fashion as discussed for the step **1$_t$** → **2$_t$**. The N_2O approach in the transition state **[1$_c$-4$_c$]**‡ is asynchronous with relatively shorter Si1—O1 distance compared to Si2—O1 (Si1—O1 = 2.282 Å *vs.* Si2—O1 = 3.547 Å). The imaginary mode in the transition state depicts the usual approach of O1 toward Si1 center with a concomitant elongation of O1—N_2 bond in N_2O. The activation barrier for this step is 31.6 kcal/mol which is lower than the barrier for the step **1$_t$** → **2$_t$** by 1.2 kcal/mol (Tables 2 and 3). The O1 atom is closer to Si1 in **[1$_t$-4$_c$]**‡ than Si2 in **[1$_t$-2$_t$]**‡ (Si1—O1 = 2.282 Å *vs.* Si2—O1 = 2.357 Å) indicating a slightly late transition state along the N_2O approaching reaction coordinate. The charge transfer from the disilene unit to the incoming N_2O at **[1$_t$-4$_c$]**‡ is 0.371 *e*. This value is lower than one observed in **[1$_t$-2$_t$]**‡ because the HOMO of **1$_c$** is more stabilized than **1$_t$** (E_{HOMO} = −4.14 eV for **1$_c$** and −3.99 eV for **1$_t$**) leading to a slightly higher energy difference. Subsequently in the final step, **4$_c$** will proceed to yield the *cis*-product **P$_c$** after addition of a second molecule of N_2O (Fig. 5), as already discussed in pathway I.

The 1,2 migration leading to silysilylene intermediate was first reported by Sakurai et al. while studying the rearrangement of transient hexamethyltrisilene to its corresponding trisilane-1,1-diyl at 200 °C [42]. We have not explored this route in this current study since the 1,2 migration of the bulky group will entail a huge activation barrier that is not feasible under ambient experimental conditions.

3.3. Pathway III

This particular pathway will focus on a completely new route involving the silanone intermediate **6** (Scheme 4, Fig. 6). The monomeric silylene **2c$_m$** formed from the dissociation of **1$_t$** can itself react with a molecule of N_2O to afford a relatively unstable intermediate **5**. We have witnessed a very interesting event during the N_2O addition to **2c$_m$**. During a linear transit scan with gradual decrease of O1—Si1 distance, there was always a bend back of the terminal N3 atom of N_2O toward Si1 (Fig. 3) [30]. With this understanding we performed another potential energy surface scan where the terminal nitrogen was bought closer to the Si1 atom instead of O1. This approach of N3 resulted in a new intermediate **5** *via* the transition state **[2c$_m$-5]**‡ (see Figs. 3 and 6). The step **2c$_m$** → **5** entails a moderately lower activation barrier of 6.5 kcal/mol ($\Delta H_{sol}{}^{L}$), however the free energy of activation ($\Delta G_{sol}{}^{L}$) shows a higher value of 16.1 kcal/mol due to the loss of vibrational contribution to the entropy. As expected, the transition state eigenvector in **[2c$_m$-5]**‡ depicts the incoming motion of N3 toward the Si1 center. The structural feature at **[2c$_m$-5]**‡ reveals that the Cp* ligand still maintains a η^2 type of bonding mode with the central Si1 atom as seen in **2c$_m$** (refer Table 1). N3 and O1 atoms are 2.507 Å and 3.535 Å away from Si1 center (Fig. 3) indicating early transition state along the Si1—N3 reaction coordinate. The bending of the N_2O moiety has resulted in decrease of O1—N—N3 bond angle (151.8°) with respect to its initial linear arrangement. Furthermore, similar to previous N_2O addition, finite charge transfer of 0.237 *e* from the silylene unit to the incoming N_2O moiety was observed. In the intermediate **5**, both the atoms O1 and N3 have progressed more closer to the Si1 center with distances of 1.729 Å and 3.127 Å respectively. However structure of the type **5** is not rare. Very recently, Severin et al. have obtained crystal structures of N_2O adduct with various substituted N-heterocyclic carbene species [43]. The structures possess a bent N_2O group linked *via* N-atom to the carbene carbon, exhibiting a coordination mode similar to **5**.

Further progress of O1 toward Si1 allowed the formation of **6** with the liberation of dinitrogen species (Scheme 4 and Fig. 6). The step **5** → **6** is barrier-less and spontaneous, witnessing a high exothermicity of -77.6 kcal/mol ($\Delta H_{sol}{}^{L}$, Table 4). Silanones of the type **6** may exist as a transient intermediate during the reaction process. In general, isolation and subsequent characterization of silanones ($R_2Si{=}O$) at room temperature remains elusive. The reason may be the polarity of the ylide-like Si=O bond allowing the more negative charge to be residing on the electronegative O atom leaving the Si center electrophilic, rendering the molecule to be more reactive. Silanones may turn out to be an important reactive intermediate in facilitating various reactions particularly in activating small molecules. Recently, Driess et al. have isolated and characterized silanones which are stabilized by N-heterocyclic carbenes [44]. They initially synthesized the NHC-silylene adduct which was then reacted with N_2O to yield the oxygenated NHC-supported silanone adduct. Motivated by their findings, the same group has studied the reactivity of DMAP stabilized silanones with ammonia affording a unique pair of tautomeric products [45]. The Si1—O1 distance in **6** is 1.568 Å, which is in close agreement with the value of 1.542(2) Å obtained from the X-ray structure of NHC supported silanone.[44] The geometry around the Si1 atom in **6** is nearly planar with the sum of bond angles around Si1 atom is 358° [46]. The planar geometry can be anticipated from the famous CGMT (Carter–Goddard–Malrieu–Trinquier) model [47]. The model states that bent geometry of $R_2Si{=}X$ compounds originates from σ^*–π mixing of orbitals and it becomes stable than planar geometry when $\sum \Delta E_{ST} > (1/2)(E_\sigma + E_\pi)$. $\sum \Delta E_{ST}$ is the sum of the singlet-triplet energy difference of the silylene and the X atom while E_σ and E_π are the σ and π bond energies of the Si=X double bond. The calculated $\sum \Delta E_{ST}$ value in **6** is −36.7 kcal/mol since the ΔE_{ST} value of oxygen in ground state triplet configuration is −64.9 kcal/mol [48], surpassing the ΔE_{ST} value of 28.2 kcal/mol [49] for **2c$_m$**. While the $E_\sigma + E_\pi$ value of **6** is calculated to be 148 kcal/mol, which is much higher than the $\sum \Delta E_{ST}$ value, it is evident that the geometry around the Si atom will be planar. A similar conclusion was reported by Kira and Iwamoto while interpreting the planar geometry around the Si atom for their stable dialkyl substituted silanechalcogenones [50].

The TD-DFT spectrum of **6** shows weak intensity absorptions at a lower wavelength regime (Table S7 and Figure S3). Excitation at 360 nm is characterized predominantly as HOMO-1 → LUMO transition, which is $n \rightarrow \pi^*$ in nature. The HOMO-1 orbital has major contributions from N1(p_x) and O3(p_y) atomic orbitals providing a non-bonding character while LUMO depicts the Si—O π^* interaction. A similar finding was reported by Tamao, Matsuo and coworkers while explaining the bonding and spectral features of the first stable germanone species [51]. Other vital transitions at

323 and 298 nm are π–π^* type (Figure S2) with oscillator strength of 0.035 and 0.044 respectively (Table S7). Kira and coworkers have reported a similar trend in spectral signatures for dialkylsilanethione species [50].

Here in pathway III there might be a possibility where the silanone **6** can react with another monomeric silylene unit $\mathbf{2c_m}$ obtained from the dissociation of the disilene $\mathbf{1_t}$. Addition of $\mathbf{2c_m}$ molecule to **6** in different orientations allowed the formation of either the *trans*-monooxadisiletane species $\mathbf{2_t}$ or its *cis*-variant $\mathbf{4_c}$ (Fig. 6). The silylene addition steps ($\mathbf{6} \rightarrow \mathbf{2_t}$ and $\mathbf{6} \rightarrow \mathbf{4_c}$) are barrier-less resulting into the desired intermediates $\mathbf{2_t}$ and $\mathbf{4_c}$, accompanying a high exothermicity of −28.0 kcal/mol and −18.1 kcal/mol respectively ($\Delta H_{sol}{}^{L}$, Table 4). Very recently, Kira, Iwamoto and coworkers have studied the reaction of dialkylsilylene with ketones giving rise to siloxirane ring products [52]. Their proposed mechanism envisages the formation of carbonyl silaylide intermediate and its existence in various canonical forms prior to cyclization. The DFT calculations performed by the authors at B3LYP/6-31G+(d) level showed the exothermicity of around −25 kcal/mol for the formation of different siloxiranes [52]. Encouragingly, the reported energy value is comparable or even higher than our calculated exothermicity values (refer Table S4 for $\Delta E_e{}^{L}$ values) for monooxadisiletane intermediate formation (*vide supra*). Further addition of a second molecule of N_2O will afford the products $\mathbf{P_t}$ and $\mathbf{P_c}$ *via* the transition states $\mathbf{[2_t\text{-}P_t]^{\ddagger}}$ and $\mathbf{[4_c\text{-}P_c]^{\ddagger}}$ respectively. The details of these steps are discussed in the previous pathways (*vide supra*).

There might exist another possibility where two silanone intermediates **6** can undergo a [2+2] cycloaddition type reaction (Scheme 4) to form the cyclic products $\mathbf{P_t}$ and $\mathbf{P_c}$ respectively. To investigate these reaction steps we allowed the gradual progress of two silanone intermediates in a manner where the substituent's are oriented either *trans*- or *cis*- with respect to each other. Unfortunately, we are unable to optimize a genuine transition state along the two similar reaction coordinates instead we obtain two intermediates **7** and **8**, where the silanone units are loosely coordinated to each other (Scheme 4, Fig. 3) with Si1—Si2 distances of 5.115 Å and 5.363 Å in **7** and **8** respectively. Both **7** and **8** are unstable than **6** by 17.9 and 15.8 kcal/mol, however such high energy values including the absence of transition states are not surprising as the Si—O bond in silanone is more polarized (*vide supra*) unlike C—O bond in ketones and hence will not follow a usual [2+2] cycloaddition reaction. Hence we can conceive a pathway where the two silanone intermediates can mutually combine to form an initial pre-complex, which can be accessed at room temperature despite being endoergic (<20 kcal/mol). Furthermore, these pre-complexes can subsequently collapse to furnish the dioxadisiletane ring products (Scheme 4, Fig. 6). This step seems to be the most preferred route since the intermediates $\mathbf{2_t}$ and $\mathbf{4_c}$ formed from **6** will require very high activation barrier (~40 kcal/mol) to combine with a second N_2O molecule and hence can be neglected. To our surprise, re-optimization of **7** and **8** at B97D/SVP level directly resulted in the products $\mathbf{P_t}$ and $\mathbf{P_c}$ respectively allowing us to apprehend that the combination of the two silanone intermediates are indeed facile. Another argument can be proposed in favor for silanone dimerization step is by pointing out the thermodynamic stability and kinetic hindrance of the monoxygenated intermediates $\mathbf{2_t}$ and $\mathbf{4_c}$ (*vide supra*). Since these intermediates were not isolated in the experimental study we can opine that reaction could have followed a different channel *via* silanone dimerization leading to the formation of the products.

Using both computational and experimental studies Leigh, Bendikov and coworkers have reported that alcohol addition to silenes occurs through a mechanism involving alcohol dimers rather than monomers [53]. The activation barrier involving dimeric alcohols are lower than the monomeric form. Very recently, Su and Li studied the mechanism of 1,2 addition of methanol to highly strained dimetallene species [14]. Their calculated results reveal that the activation barrier involving two methanol molecules are substantially lower than the one involving single methanol molecule. To this end, we decided to check the effect of disilene oxygenation in presence of two N_2O molecules. The attack of two N_2O molecules to $\mathbf{1_t}$ can either occur from both sides or from opposite sides of the Si=Si bond. The gradual attack of N_2O molecules toward silicon atoms from the same side resulted in the cleavage of the Si1—Si2 bond with formation of two molecules of silanones and liberation of nitrogen molecules. The PES scan of the impingement of two N_2O molecules from the same side is depicted in Figure S6. It is observed that the Si1—Si2 bond ruptures (Si1—Si2 ~5.1 Å) early during the scan, with two N_2Os away from the silicon centers by 3.5 Å. Unfortunately, this transformation involving the addition of two N_2Os from the same side is energy demanding (~63.4 kcal/mol) and hence it can be conceivable that the silylenes formed after the early dissociation of $\mathbf{1_t}$ can undergo N_2O addition independently following the step $\mathbf{2c_m} \rightarrow \mathbf{5}$ as illustrated in pathway III (*vide supra*). On the other hand the attack of N_2O molecules from the opposite sides allows the formation of monooxadisiletane ring product without any coordination from the second N_2O molecule. This result however prompted us to anticipate that the addition of N_2O molecules to $\mathbf{1_t}$ from the opposite should occur in a stepwise fashion as demonstrated in the studied pathways (*vide supra*).

4. Conclusion

In this work, we have used DFT to unravel the mechanistic routes for disilene activation in presence of N_2O. Three different pathways were investigated for disilene oxidation resulting in the formation of both *trans*-dioxadisiletane and *cis*-dioxadisiletane products as displayed in Scheme 1. In pathway I, reaction of N_2O with $\mathbf{1_t}$ furnished the monoxygenated product $\mathbf{2_t}$, which subsequently added second N_2O molecule resulting in the formation of the major product $\mathbf{P_t}$. In the same pathway we have studied the transformation of $\mathbf{2_t}$ to the *cis*-monoxygenated intermediate $\mathbf{4_c}$. Subsequent oxygenation with the second N_2O afforded the *cis*-product $\mathbf{P_c}$. The isomerization step from $\mathbf{2_t} \rightarrow \mathbf{4_c}$ was accomplished by initial Si1—Si2 bond cleavage and subsequent rotation around the O1—Si2 bond. The next reaction channel, pathway II, deals with the possibility of isomerization prior to the N_2O additions. For the first time a thorough computational investigation was carried out to explore the different routes for disilene isomerization. The dissociation-recombination mechanism along with the single-step rotation around the Si1—Si2 were studied, the energetics for both the steps were compared in pathway II. The *cis*-disilene $\mathbf{1_c}$ formed after the isomerization can sequentially add two N_2O molecules resulting in $\mathbf{4_c}$ and $\mathbf{P_c}$ respectively, analogous to its *trans*-variant $\mathbf{2_t}$ and $\mathbf{P_t}$. In the final route, pathway III, we have discussed about the formation of the transient silanone species **6**, after reaction of N_2O with monomeric silylene moiety $\mathbf{2c_m}$. The intermediate **6** will further react with another silanone unit, to afford either intermediate **7** or **8**. Intermediates **7** and **8** are loosely coordinated complexes, with Cp* and $[(Me_3Si)_2N]$ substituents coordinated either *trans*- or *cis*- to each other. Subsequent combination of the silanone fragments in **7** and **8** will give rise to the desired products. Importantly, the formation of *trans*-dioxadisiletane product $\mathbf{P_t}$ is more favorable than the isomeric *cis*-dioxadisiletane $\mathbf{P_c}$, a finding in accordance with the experimental observation. Furthermore, calculated energy profiles reveal that pathway III will undergo energetically facile transformation compared to other pathways and can be conceived under the normal reaction condition. Hence we envisage that pathway III might be the most viable reaction channel nevertheless the other pathways studied cannot directly be overruled. We also

encourage the experimental researchers to further investigate the reaction and isolate intermediates to provide more insight to our mechanistic predictions.

Acknowledgements

BM acknowledges CSIR for the JRF fellowship. The authors acknowledge IISER-Kolkata for the computational facility. DK is grateful to the DST-SERB for the fast-track fellowship (No: SR/FT/CS-72/2011) and IISER-Kolkata for the start-up grant. The authors are grateful to the reviewers for providing fruitful suggestions.

Appendix A. Supplementary data

Supplementary data associated with this article can be found, in the online version, at http://dx.doi.org/10.1016/j.jmgm.2014.04.011.

References

[1] R. West, M.J. Fink, J. Michl, Tetramesityldisilene, a stable compound containing a silicon–silicon double bond, Science 214 (1981) 1343–1344.
[2] (a) M. Weidenbruch, in: Z. Rappoport, Y. Apeloig (Eds.), The Chemistry of Organosilicon Compounds, vol. 3, Wiley, Chichester, UK, 2001, pp. 391–428;
(b) T. Muller, W. Ziche, N. Auner, in: Z. Rappoport, Y. Apeloig (Eds.), The Chemistry of Organic Silicon Compounds, vol. 2, New York, Wiley, 1998, p. 857;
(c) R. Okazaki, R. West, Chemistry of stable disilenes, Adv. Organomet. Chem. 39 (1996) 231–273;
(d) M. Kira, T. Iwamoto, Progress in the chemistry of stable disilenes, Adv. Organomet. Chem. 54 (2006) 73–148;
(e) M. Kira, Isolable silylene, disilenes, trisilaallene, and related compounds, J. Organomet. Chem. 689 (2004) 4475–4488;
(f) A.G. Brook, M.A. Brook, The chemistry of silenes, Adv. Organomet. Chem. 39 (1996) 71–158;
(g) J. Escudié, C. Couret, H. Ranaivonjatovo, Silenes >Si—C<, germenes >Ge═C< and stannenes >Sn═C< The French contribution, Coord. Chem. Rev. 180 (1998) 565–592;
(h) M. Weidenbruch, Silylenes and disilenes: examples of low coordinated silicon compounds, Coord. Chem. Rev. 130 (1994) 275–300;
(i) R. West, Chemistry of the silicon–silicon double bond, Angew. Chem. Int. Ed. Engl. 26 (1987) 1201–1220;
(j) N. Wiberg, W. Niedermayer, K. Polborn, P. Mayer, Reactivity of the isolable disilene R*PhSi═SiPhR*(R*═SitBu3), Chem. Eur. J. 8 (2002) 2730–2739, and references therein.
[3] (a) N. Tokitoh, H. Suzuki, R. Okazaki, K. Ogawa, Synthesis, structure, and reactivity of extremely hindered disilenes: the first example of thermal dissociation of a disilene into a silylene, J. Am. Chem. Soc. 115 (1993) 10428–10429;
(b) N. Takeda, N. Tokitoh, A bulky silylene generated under mild conditions: its application to the synthesis of organosilicon compounds, Synlett (2007) 2483–2491;
(c) H. Suzuki, N. Tokitoh, R. Okazaki, J. Harada, K. Ogawa, S. Tomoda, M. Goto, Synthesis and structures of extremely hindered and stable disilenes, Organometallics 14 (1995) 1016–1022.
[4] S. Tsutsui, H. Tanaka, E. Kwon, S. Matsumoto, K. Sakamoto, Thermal equilibrium between a lattice-framework disilene and the corresponding silylene, Organometallics 23 (2004) 5659–5661.
[5] S. Tsutsui, K. Sakamoto, M. Kira, Bis(diisopropylamino)silylene and its dimer, J. Am. Chem. Soc. 120 (1998) 9955–9956.
[6] T.A. Schmedake, M. Haaf, Y. Apeloig, T. Müller, S. Bukalov, R. West, Reversible transformation between a diaminosilylene and a novel disilene, J. Am. Chem. Soc. 121 (1999) 9479–9480.
[7] P. Jutzi, A. Mix, B. Neumann, B. Rummel, W.W. Schoeller, H.-G. Stammler, A.B. Rozhenko, Reversible transformation of a stable monomeric silicon(II) compound into a stable disilene by phase transfer: experimental and theoretical studies of the system $\{[(Me_3Si)_2N](Me_5C_5)Si\}_n$ with $n = 1,2$, J. Am. Chem. Soc. 131 (2009) 12137–12143.
[8] S. Khan, S.S. Sen, H.W. Roesky, D. Kratzert, R. Michel, D. Stalke, One pot synthesis of disilatricycloheptene analogue and Jutzi's disilene, Inorg. Chem. 49 (2010) 9689–9693.
[9] (a) S. Khan, R. Michel, D. Koley, H.W. Roesky, D. Stalke, Reactivity studies of a disilene with N_2O and elemental sulfur, Inorg. Chem. 50 (2011) 10878–10883;
(b) S. Khan, R. Michel, S.S. Sen, S.H.W. Roesky, D. Stalke, A P4 chain and cage from silylene-activated white phosphorous, Angew. Chem. Int. Ed. 50 (2011) 11786–11789.
[10] (a) M. Weidenbruch, Some silicon, germanium, tin and lead analogues of carbenes, alkenes and dienes, Eur. J. Inorg. Chem. (1999) 373–381;
(b) M. Haaf, T.A. Schmedake, R. West, Stable Silylenes, Acc. Chem. Res. 33 (2000) 704–714;
(c) B. Gehrhus, P.B. Hitchcock, H. Jansen, The stable silylene Si[$(NCH_2Bu^t)_2C_6H_4$-1,2]: reactions with group 14 element halides, J. Organomet. Chem. 691 (2006) 811–816;
(d) M. Kira, T. Iwamoto, Stable cyclic and acyclic persilyldisilenes, J. Organomet. Chem. 611 (2000) 236–247;
(e) R. West, Multiple bonds to silicon: 20 years later, Polyhedron 21 (2002) 467–472;
(f) M. Weidenbruch, Some recent advances in the chemistry of silicon and its homologues in low coordination states, J. Organomet. Chem. 646 (2002) 39–52;
(g) M. Weidenbruch, From a cyclotrisilane to a cyclotriplumbane: low coordination and multiple bonding in group 14 chemistry, Organometallics 22 (2003) 4348–4360;
(h) N.J. Hill, R. West, Recent developments in the chemistry of stable silylenes, J. Organomet. Chem. 689 (2004) 4165–4183;
(i) M. Kira, An isolable dialkylsilylene and its derivatives, A step toward comprehension of heavy unsaturated bonds, Chem. Commun. 46 (2010) 2893–2903;
(j) V.Y. Lee, A. Sekiguchi, Aromaticity of group 14 organometallics: experimental aspects, Angew. Chem. Int. Ed. 46 (2007) 6596–6620;
(k) A. Sekiguchi, M. Ichinohe, R. Kinjo, The chemistry of disilyne with a genuine Si—Si triple bond: synthesis, structure and reactivity, Bull. Chem. Soc. Jpn. 79 (2006) 825–832;
(l) N. Wiberg, Sterically overloaded supersilylate main group elements and main group element clusters, Coord. Chem. Rev. 163 (1997) 217–252;
(m) P.P. Power, Homonuclear multiple bonding in heavier main group elements, J. Chem. Soc., Dalton Trans. (1998) 2939–2951;
(n) Kira.F M., T. Iwamoto, S. Ishida, in: N. Auner, J. Weis (Eds.), Organosilicon Chemistry VI-from Molecules to Materials, Wiley-VCH, Weinheim, 2005, p. 25;
(o) N. Wiberg, W. Niedermayer, K. Polborn, H. Nöth, J. Knizek, D. Fenske, G.G. Baum, in: N. Auner, J. Weis (Eds.), Organosilicon Chemistry IV, Wiley-VCH, Weinheim, 2000, p. 93;
(p) R.S. Ghadwal, R. Azhakar, H.W. Roesky, Dichlorosilylene: a high temperature transient species to an indispensable building block, Acc. Chem. Res. 46 (2013) 444–456;
(q) H. Joo, M.L. McKee, Computational study of the "stable" bis(amino)silylene reaction with halomethanes. A radical or concerted mechanism? J. Phys. Chem. A 109 (2005) 3728–3738;
(r) R.-E. Li, J.-H. Sheu, M.-D. Su, Reactivity and mechanism of stable heterocyclic silylenes with carbon tetrachloride, Inorg. Chem. 46 (2007) 9245–9253;
(s) B.H. Boo, S. Im, S. Lee, Ab initio and DFT studies of the thermal rearrangement of trimethylsilyl(methyl)silylene: remarkable rearrangements of silicon intermediates, J. Comput. Chem. 31 (2010) 154–163.
[11] (a) Y. Apeloig, T. Müller, Do silylenes always dimerize to disilenes? Novel silylene dimers with unusual structures, J. Am. Chem. Soc. 117 (1995) 5363–5364;
(b) T. Müller, Y. Apeloig, Possible strategies toward the elusive tetraaminodisilene, J. Am. Chem. Soc. 124 (2002) 3457–3460;
(c) M. Driess, S. Yao, M. Brym, C. van Wüllen, D. Lentz, A new type of N-heterocyclic silylene with ambivalent reactivity, J. Am. Chem. Soc. 128 (2006) 9628–9629;
(d) M. Kira, S. Ishida, T. Iwamoto, C. Kabuto, The first isolable dialkylsilylene, J. Am. Chem. Soc. 121 (1999) 9722–9723;
(e) C.W. So, H.W. Roesky, P.M. Gurubasavaraj, R.B. Oswald, M.T. Gamer, P.G. Jones, S. Blaurock, Synthesis and structures of heteroleptic silylenes, J. Am. Chem. Soc. 129 (2007) 12049–12054;
(f) M. Denk, R. Lennon, R. Hayashi, R. West, A. Haaland, H. Belyakov, P. Verne, M. Wagner, N. Metzler, Synthesis and structure of a stable silylene, J. Am. Chem. Soc. 116 (1994) 2691–2692;
(g) S. Yao, M. Brym, C. van Wüllen, M. Driess, Synthesis and characterization of [PhC(N*t*Bu2]SiCl: a stable monomeric chlorosilylene, Angew. Chem. Int. Ed. 45 (2006) 3948–3950;
(h) P. Jutzi, K. Leszczyñska, B. Neumann, W.W. Schoeller, H.-G. Stammler, [2,6-(Trip)2H3C6](Cp*)Si: a stable monomeric arylsilicon(II) compound, Angew. Chem. Int. Ed. 48 (2009) 2596–2599;
(i) H. Jacobsen, T. Ziegler, Nonclassical double bonds in ethylene analogs: influence of Pauli repulsion on trans bending and pi-bond strength. A density functional study, J. Am. Chem. Soc. 116 (1994) 3667–3679;
(j) M. Karni, Y. Apeloig, Substituent effects on the geometries and energies of the silicon–silicon double bond, J. Am. Chem. Soc. 112 (1990) 8589–8590;
(k) C. Liang, L.C. Allen, Group IV double bonds: shape deformation and substituent effects, J. Am. Chem. Soc. 112 (1990) 1039–1041;
(l) H. Teramae, Ab initio studies on a silicon compound. The electronic structure of disilene reconsidered, J. Am. Chem. Soc. 109 (1987) 4140–4142;
(m) M.S. Gordon, D. Bartol, Molecular and electronic structure of Si_3H_6, J. Am. Chem. Soc. 109 (1987) 5948–5950;
(n) M.C. Holthausen, W. Koch, Y. Apeloig, Theory predicts triplet ground-state organic silylenes, J. Am. Chem. Soc. 121 (1999) 2623–2624;
(o) M. Asay, S. Inoue, M. Driess, Aromatic ylide-stabilized carbocyclic silylene, Angew. Chem. Int. Ed. 50 (2011) 9589–9592;
(p) R.S. Ghadwal, H.W. Roesky, S. Merkel, J. Henn, D. Stalke, Lewis base stabilized dichlorosilylene, Angew. Chem. Int. Ed. 48 (2009) 5683–5686;
(q) Y. Wang, Y. Xie, P. Wei, B. King, H.F. Schaefer III, R.P.V Schleyer, G.H. Robinson, A stable silicon(0) compound with a Si═Si double bond, Science 321 (2008) 1069;
(r) K. Abersfelder, A.J.P. White, H.S. Rzepa, D. Scheschkewitz, A tricyclic aromatic isomer of hexasilabenzene, Science 327 (2010) 564–566.
[12] (a) B. Hajgató, M. Takahashi, M. Kira, T. Veszprémi, The mechanism of 1,2-addition of disilene and silene: hydrogen halide addition, Chem. Eur. J. 8 (2002)

2126–2133;
(b) M. Takahashi, T. Veszprémi, B. Hajgató, M. Kira, Theoretical study on stereochemical diversity in the addition of water to sisilene, Organometallics 19 (2000) 4660–4662;
(c) T. Veszprémi, M. Takahashi, J. Ogasawara, K. Sakamoto, M. Kira, An ab initio MO study of structure and reactivity of 4-silatriafulvene, J. Am. Chem. Soc. 120 (1998) 2408–2414;
(d) M. Takahashi, T. Veszprémi, M. Kira, Importance of frontier orbital interactions in addition reaction of water to disilene, Int. J. Quantum Chem. 84 (2001) 192–197;
(e) T. Veszprémi, M. Takahashi, B. Hajgató, M. Kira, The mechanism of 1,2-addition of disilene and silene. 1. Water and alcohol addition, J. Am. Chem. Soc. 123 (2001) 6629–6638;
(f) Y. Apeloig, M. Nakash, The mechanism of addition of phenols to tetramesityldisilene. Evidence for both nucleophilic and electrophilic rate-determining steps, J. Am. Chem. Soc. 118 (1996) 9798–9799;
(g) Y. Apeloig, M. Nakash, Solvent-dependent stereoselectivity in the addition of p-CH3OC6H4OH to (E)-1,2-di-tert-butyl-1,2-dimesityldisilene. Evidence for rotation around the Si—Si bond in the zwitterionic intermediate, Organometallics 17 (1998) 1260–1265;
(h) Y. Apeloig, M. Nakash, Arrhenius parameters for the addition of phenols to the silicon–silicon double bond of tetramesityldisilene, Organometallics 17 (1996) 2307–2312.

[13] (a) B.-Y. Li, M.-D. Su, Theoretical investigations of the reactions of phosphino disilenes and their derivatives with an E═E (E = C, Si, Ge, Sn, and Pb) double bond, J. Phys. Chem. A 116 (2012) 9412–9420;
(b) B.-Y. Li, J.-H. Sheu, M.-D. Su, Mechanisms for the reaction of water, butadiene, and palladium complex with 1,2-dimetallacyclohexene (R_2M═MR_2, M = C, Si, Ge, Sn, Pb). A theoretical study, Organometallics 30 (2011) 4862–4872.

[14] B.-Y. Li, M.-D. Su, Theoretical investigation of the mechanisms for the reaction of fused tricyclic dimetallenes containing highly strained E═E (E = C, Si, Ge, Sn, and Pb) double bonds, J. Phys. Chem. A 116 (2012) 4222–4232.

[15] J. Hansen, M. Sato, Greenhouse gas growth rates, Proc. Natl. Acad. Sci. U S A 101 (2004) 16109–16114.

[16] P. Chen, S.I. Gorelsky, S. Ghosh, E.I. Solomon, N_2O reduction by the μ_4-sulfide-bridged tetranuclear Cu_z cluster active site, Angew. Chem. Int. Ed. 43 (2004) 4132–4140.

[17] (a) J.-H. Lee, M. Pink, J. Tomaszewski, H. Fan., K.G. Caulton, Facile hydrogenation of N_2O by an operationally unsaturated osmium polyhydride, J. Am. Chem. Soc. 129 (2007) 8706–8707;
(b) G.A. Vaughan, P.B. Rupert, G.L. Hillhouse, Selective O-atom transfer from nitrous oxide to hydride and aryl ligands of bis(pentamethylcyclopentadienyl)hafnium derivatives, J. Am. Chem. Soc. 109 (1987) 5538–5539;
(c) G.A. Vaughan, C.D. Sofield, G.L. Hillhouse, A.L. Rheingold, Oxygen-atom transfer from nitrous oxide. Identification of intermediates in the oxidation of diphenylacetylene at group 4 metal centers and the structural characterization of (η-C5Me5)2Ti{N(O)NCPh═CPh}•1/2C7H8, J. Am. Chem. Soc. 111 (1989) 5491–5493;
(d) G.A. Vaughan, G.L. Hillhouse, A.L. Rheingold, Syntheses, structures, and reactivities of unusual four-membered metallacycles formed in insertion reactions of N═N═O, N═N═NR, and N═N═CR_2 with (η^5-C_5Me_5)$_2$Zr(C_2Ph_2), J. Am. Chem. Soc. 112 (1990) 7994–8001;
(e) A.W. Kaplan, R.G. Bergman, Nitrous oxide mediated oxygen atom insertion into a ruthenium–hydride bond. Synthesis and reactivity of the monomeric hydroxoruthenium complex $(DMPE)_2Ru(H)(OH)$, Organometallics 16 (1997) 1106–1108;
(f) H.Z. Yu, G.C. Jia, Z.Y. Lin, DFT studies on the mechanism of reactions between N_2O and $Cp_2M(\eta^2$-alkyne) (M = Ti, Zr), Organometallics 26 (2007) 6769–6777;
(g) H.Z. Yu, G.C. Jia, Z.Y. Lin, Theoretical studies on O-insertion reactions of nitrous oxide with ruthenium hydride complexes, Organometallics 27 (2008) 3825–3833;
(h) F. Bottomley, Cyclopentadienylmetal oxides, Polyhedron 11 (1992) 1707–1731;
(i) W.A. Howard, G. Parkin, Terminal oxo, sulfido, selenido, and tellurido complexes of zirconium, (η^5-C_5Me_4R)$_2$Zr(E)(NC_5H_5): comparison of terminal Zr—E single and Zr═E double-bond lengths, J. Am. Chem. Soc. 116 (1994) 606–615;
(j) W.H. Harman, C.J. Chang, N_2O activation and oxidation reactivity from a non-heme iron pyrrole platform, J. Am. Chem. Soc. 129 (2007) 15128–15129;
(k) C.E. Laplaza, A.L. Odom, W.M. Davis, C.C. Cummins, J.D. Protasiewicz, Cleavage of the nitrous oxide NN bond by a tris(amido)molybdenum(III) complex, J. Am. Chem. Soc. 117 (1995) 4999–5000;
(l) A.R. Johnson, W.M. Davis, C.C. Cummins, S. Serron, S.P. Nolan, D.G. Musaev, K. Morokuma, Four-coordinate molybdenum chalcogenide complexes relevant to nitrous oxide N—N bond cleavage by three-coordinate molybdenum(III): synthesis, characterization, reactivity, and thermochemistry, J. Am. Chem. Soc. 120 (1998) 2071–2085;
(m) J.-P.F. Cherry, A.R. Johnson, L.M. Baraldo, Y.-C. Tsai, C.C. Cummins, S.V. Kryatov, E.V. Rybak-Akimova, K.B. Capps, C.D. Hoff, C.M. Haar, S.P. Nolan, On the origin of selective nitrous oxide N—N bond cleavage by three-coordinate molybdenum(III) complexes, J. Am. Chem. Soc. 123 (2001) 7271–7286.

[18] M.J. Frisch, et al., Gaussian-03, Revision E.01, Gaussian, Inc., Wallingford, CT, 2004.

[19] M.J. Frisch, et al., Gaussian-09, Revision C.01, Gaussian, Inc., Wallingford, CT, 2009.

[20] A.D. Becke, Density-functional exchange-energy approximation with correct asymptotic behavior, Phys. Rev. A 38 (1988) 3098–3100.

[21] (a) J.P. Perdew, Density-functional approximation for the correction energy of the inhomogeneous electron gas, Phys. Rev. B 33 (1986) 8822–8824;
(b) J.P. Perdew, Density-functional approximation for the correction energy of the inhomogeneous electron gas, Phys. Rev. B 34 (1986) 7406.

[22] A. Schäfer, H. Horn, R. Ahlrichs, Fully optimized contracted Gaussian basis sets for atoms Li to Kr, J. Chem. Phys. 97 (1992) 2571–2577.

[23] (a) B.I. Dunlap, Fitting the coulomb potential variationally in Xα molecular calculations, J. Chem. Phys. 78 (1983) 3140–3142;
(b) B.I. Dunlap, Robust and variational fitting: removing the four-center integrals from center stage in quantum chemistry, J. Mol. Struct. (Theochem) 529 (2000) 37–40.

[24] F. Weigend, R. Ahlrichs, Balanced basis sets of split valence, triple zeta valence and quadruple zeta valence quality for H to Rn: design and assessment of accuracy, Phys. Chem. Chem. Phys. 7 (2005) 3297–3305.

[25] (a) S. Grimme, Semiempirical GGA-type density functional constructed with a long-range dispersion correction, J. Comp. Chem. 27 (2006) 1787–1799;
(b) A.D. Becke, Density-functional thermochemistry. V. Systematic optimization of exchange-correlation functional, J. Chem. Phys. 107 (1997) 8554–8560.

[26] A.V. Marenich, C.J. Cramer, D.G. Truhlar, Universal solvation model based on solute electron density and on a continuum model of the solvent defined by the bulk dielectric constant and atomic surface tensions, J. Phys. Chem. B 113 (2009) 6378–6396.

[27] Y. Zhao, D.G. Truhlar, The M06 suite of density functional for main group thermochemistry, thermochemical kinetics, noncovalent interactions, excited states, and transition elements: two new functional and systematic testing of four M06-class functional and 12 other functional, Theor. Chem. Acc. 120 (2008) 215–241.

[28] A.E. Reed, L.A. Curtiss, F. Weinhold, Intermolecular interactions from a natural bond orbital, donor–acceptor viewpoint, Chem. Rev. 88 (1998) 899–926.

[29] http://www.chemcraftprog.com/index.html.

[30] On the contrary, we have performed calculations where N_2O approaches to only one silicon atom (Si_2, Figure S4). Interestingly this exercise resulted to a peculiar structure where the N2 fragment of N_2O bends towards the other silicon center. This is also not surprisingly since the LUMO of N_2O contains appreciate contribution from the terminal nitrogen atom as evident from Figure 2. This structure later resulted to the cleavage of Si1—Si2 bond giving rise to a silanone and a silylene unit having loose interaction with the decoordinated N_2. However, even after repeated attempts we could not designate a proper transition state for this transformation.

[31] (a) K. Fukui, Recognition of stereochemical paths by orbital interaction, Acc. Chem. Res. 4 (1971) 57–64;
(b) I. Fleming, Frontier Orbital and Organic Chemical Reactions, Wiley-Interscience, New York, 1976.

[32] M.D. Harmony, V.W. Laurie, R.L. Kuczkowski, R.H. Schwendeman, D.A. Ramsay, F.J. Lovas, W.J. Lafferty, A.G. Maki, Molecular structures of gas-phase polyatomic molecules determined by spectroscopic methods, J. Phys. Chem. Ref. Data 8 (1979) 619–721.

[33] (a) R.S. Grev, H.F. Schaefer III, Hetero-substituted cyclopolysilanes. Unusual structures and a new model of bonding in 1,3-disubstituted four-membered rings, J. Am. Chem. Soc. 109 (1987) 6577–6585;
(b) C. Liang, L.C. Allen, σ-Bridged-π bonding in small-ring compounds, J. Am. Chem. Soc. 113 (1991) 1878–1884;
(c) D. Cremer, E. Kraka, Theoretical determination of molecular structure and conformation. 15. Three-membered rings: bent bonds, ring strain, and surface delocalization, J. Am. Chem. Soc. 107 (1985) 3800–3810;
(d) T. Kudo, S. Nagase, Theoretical study on the dimerization of silanone and the properties of the polymeric products $(H_2SiO)_n$ (n = 2, 3, and 4). Comparison with dimers $(H_2SiS)_2$ and $(H_2CO)_2$, J. Am. Chem. Soc. 107 (1985) 2589–2595;
(e) J. Ma, S. Inagaki, Cyclic delocalization of the oxygen lone pair electrons in the unusual structures of disilaoxirane and 1,3-cyclodisiloxane, J. Phys. Chem. A 104 (2000) 8989–8994, and references therein.

[34] This observation in sense will not effect the overall understanding of the pathway. The energetics for the step **2t** → **3t** (**3c** → **4c**) will not be the controlling factor for the disilene activation.

[35] (a) K. Kimura, M. Kubo, Structures of dimethyl ether and methyl alcohol, J. Chem. Phys. 30 (1959) 151–158;
(b) A. Almennigen, O. Bastiansen, V. Ewing, K. Hedberg, M. Traetteberg, The molecular structure of disiloxane (SiH3)2O, Acta Chem. Scand. 17 (1963) 2455–2460.

[36] Optimizations of **3t** and **3c** were performed for both triplet and singlet biradical type electronic states at BP86/SVP level. It was observed that the optimized triplet configuration is less stable than the singlet state (ΔE_{ST} = 3.25 kcal/mol for **3t** and 0.84 kcal/mol for **3c**) and furthermore the optimization of the singlet biradical wavefunction resulted in the closed shell singlet state. Though the ΔE_{ST} values are low we have only explored the singlet potential energy surfaces in the present study.

[37] M.-D. Su, S.-Y. Chu, Theoretical studies of the additions of germylenes to ethylene, J. Am. Chem. Soc. 121 (1999) 11478–11485.

[38] (a) B.D. Shepherd, D.R. Powell, R. West, Synthesis, geometrical isomerism, and crystal structure of a highly hindered disilene, Organometallics 8 (1989) 2664–2669;
(b) M. Kira, S. Ohya, T. Iwamoto, M. Ichinohe, C. Kabuto, Facile rotation around Si═Si double bonds in Tetrakis(trialkylsilyl)disilenes, Organometallics 19 (2000) 1817–1819;

(c) M.J. Michalczyk, R. West, J. Michl, Kinetics of thermal cis-trans isomerization in disilenes, Organometallics 4 (1985) 826–829.

[39] (a) M.W. Schmidt, P.N. Truong, M.S. Gordon, π Bond strengths in the second and third periods, J. Am. Chem. Soc. 109 (1987) 5217–5227;
(b) W. Kutzelnigg, Chemical bonding in higher main group elements, Angew. Chem. Int. Ed. Engl. 23 (1984) 272–295;
(c) G. Olbrich, P. Potzinger, B. Reimann, R. Walsh, Decomposition channels of chemically activated disilane. The π bond energy of disilene and its derivatives, Organometallics 3 (1984) 1267–1272;
(d) H.J. Kohler, H. Lischka, A systematic investigation on the structure and stability of the lowest singlet and triplet states of Si_2H_4 and SiH_3SiH and the carbon analogous compounds SiH_2CH_2, SiH_3CH, CH_3SiH, C_2H_4, and CH_3CH, J. Am. Chem. Soc. 104 (1982) 5884–5889.

[40] Ab initio calculations predicted the Si—Siπ bond strength in $H_2Si{=}SiH_2$ to be 22–28 kcal/mol [39]. This value is in proximity with our calculated result at BP86/TZVP//BP86/SVP level for **1t**. However no proper potential energy surface scan was performed and the transition state was optimized from a structure presumed to at 90° twisted configuration around the Si=Si double bond.

[41] G. Olbrich, P. Potzinger, B. Reimann, Decomposition channels of chemically activated disilane. The pi bond energy of disilene and its derivatives, Organometallics 3 (1984) 1267–1272.

[42] H. Sakurai, H. Sakaba, Y. Nakadaira, Facile preparation of 2,3-benzo-1,4-diphenyl-7-silanorbornadiene derivatives and the first clear evidence of silylene-to-disilene thermal rearrangement, J. Am. Chem. Soc. 104 (1982) 6156–6158.

[43] A.G. Tskhovrebov, B. Vuichoud, E. Solari, R. Scopelliti, K. Severin, Adducts of nitrous oxide and N-heterocyclic carbenes: syntheses, structures, and reactivity, J. Am. Chem. Soc. 135 (2013) 9486–9492.

[44] Y. Xiong, S. Yao, M. Driess, An isolable NHC-supported silanone, J. Am. Chem. Soc. 131 (2009) 7562–7563.

[45] Y. Xiong, S. Yao, R. Müller, M. Kaupp, M. Driess, Activation of ammonia by a Si=O double bond and formation of a unique pair of sila-hemiaminal and silanoic amide tautomers, J. Am. Chem. Soc. 132 (2010) 6912–6913.

[46] The sum of the angles are: [{∠(centre of mass of η^2 carbons)Si1N1} + {∠N1Si1O1} + {∠O1Si1(centre of mass of η^2 carbons)}].

[47] (a) G. Trinquier, J.P. Malrieu, P. Riviere, Unusual bonding in trans-bent digermene, J. Am. Chem. Soc. 104 (1982) 4529–4533;
(b) E.A. Carter, W.A. Goddard III, Relation between singlet-triplet gaps and bond energies, J. Phys. Chem. 90 (1986) 998–1001;
(c) G. Trinquier, J.P. Malrieu, Nonclassical distortions at multiple bonds, J. Am. Chem. Soc. 109 (1987) 5303–5315;
(d) G. Trinquier, J.P. Malrieu, in: S. Patai (Ed.), The Chemistry of Functional Group, Supplement A; The chemistry of Double-Bonded Functional Group, vol. 2, Wiley, Chichester, UK, 1989, Part 1;
(e) G. Trinquier, Double bonds and bridged structures in the heavier analogs of ethylene, J. Am. Chem. Soc. 112 (1990) 2130–2137;
(f) G. Trinquier, J.P. Malrieu, Trans bending at double bonds: scrutiny of various rationales through valence-bond analysis, J. Phys. Chem. 94 (1990) 6184–6196;
(g) J.P. Malrieu, G. Trinquier, Trans-bending at double bonds. Occurrence and extent, J. Am. Chem. Soc. 111 (1989) 5916–5921.

[48] R. Okazaki, N. Tokitoh, Heavy ketones, the heavier element congeners of a ketone, Acc. Chem. Res. 33 (2000) 625–630.

[49] R.S. Grev, H.F. Schaefer III, The ultraviolet spectrum of dimethylsilylene, J. Am. Chem. Soc. 108 (1986) 5804–5808.

[50] T. Iwamoto, K. Sato, S. Ishida, C. Kabuto, M. Kira, Synthesis, properties, and reactions of a series of stable dialkyl-substituted silicon–chalcogen doubly bonded compounds, J. Am. Chem. Soc. 128 (2006) 16914–16920.

[51] L. Li, T. Fukawa, T. Matsuo, D. Hashizume, H. Fueno, K. Tanaka, K. Tamao, A stable germanone as the first isolated heavy ketone with a terminal oxygen atom, Nature Chem. 4 (2012) 361–365.

[52] S. Ishida, T. Iwamoto, M. Kira, Reactions of an isolable dialkylsilylene with ketones, Organometallics 29 (2010) 5526–5534.

[53] W.J. Leigh, T.R. Owens, M. Bendikov, S.S. Zade, Y. Apeloig, A combined experimental and theoretical study of the kinetics and mechanism of the addition of alcohols to electronically stabilized silenes: a new mechanism for the addition of alcohols to the Si=C bond, J. Am. Chem. Soc. 128 (2006) 10772–10783.